Atmospheric processes of organic pollutants over a remote lake of the central Tibetan Plateau: Implications for regional cycling

Jiao Ren[1,3], Xiaoping Wang[1,2,*], Chuanfei Wang[1,2], Ping Gong[1,2], and Tandong Yao[1,2]

[1]Key Laboratory of Tibetan Environment Changes and Land Surface Processes, Institute of Tibetan Plateau Research, Chinese Academy of Sciences, Beijing, 100101, China

[2]CAS Center for Excellence in Tibetan Plateau Earth Sciences, Beijing, 100101, China

[3]University of Chinese Academy of Sciences, Beijing 100049, China

* Corresponding author.

(Xiaoping Wang)

E-mail: wangxp@itpcas.ac.cn

Tel: +86-10-84097120

Fax: +86-10-84097079

Abstract

Atmospheric processes (air-surface exchange, and atmospheric deposition and degradation) are crucial for understanding the global cycling and fate of organic pollutants (OPs). However, such assessment over the Tibetan Plateau (TP) remains uncertain. More than 50% of the Chinese lakes is located on the TP, which exerts a remarkable influence on the regional water, energy, and chemical cycling. In this study, air and water samples were simultaneously collected in Nam Co, a large lake on the TP, to test whether the lake is a "secondary source" or "sink" of OPs. Lower concentrations of organochlorine pesticides (OCPs) and polychlorinated biphenyls (PCBs) were observed in the atmosphere and lake water of Nam Co, while the levels of polycyclic aromatic hydrocarbons (PAHs) were relatively higher. Results of fugacity ratios and chiral signatures both suggest that the lake acted as the net sink of atmospheric hexachlorocyclohexanes (HCHs), following their long-range transport driven by the Indian Monsoon. Different behaviors were observed in the PAHs, which primarily originated from local biomass burning. Acenaphthylene, acenaphthene, and fluorene showed volatilization from the lake to the atmosphere; while other PAHs were deposited into the lake due to the integrated deposition process (wet/dry and air-water gas deposition) and limited atmospheric degradation. As the dominant PAH compound, phenanthrene exhibited a seasonal reversal of air-water gas exchange, which was likely related to the melting of the lake ice in May. The annual input of HCHs from air to the entire lake area (2015 km^2) was estimated as 1.9 kg $year^{-1}$, while those estimated for $\sum_{15}$PAHs can potentially reach up to 550 kg $year^{-1}$. This study highlights the significance of PAH deposition on the regional carbon cycling in the oligotrophic lakes of the TP.

1. Introduction

Since the past century, large quantities of organic pollutants (OPs), such as organochlorine pesticides (OCPs), polychlorinated biphenyls (PCBs), and polycyclic aromatic hydrocarbons (PAHs), have been discharged into the global environment. Soils, water bodies, and snow/ice are generally considered as reservoirs or sinks of these pollutants (Dalla Valle et al., 2005; Froescheis et al., 2000; Guglielmo et al., 2012). However, due to the influence of global warming (Komprda et al., 2013; Noyes et al., 2009), growing evidence indicates that OPs previously stored in reservoirs can be re-released back to the environment (Ma et al., 2011). For example, air-soil exchange of OCPs has showed the re-emission of OCPs from past contaminated soils in Europe (Ruzickova et al., 2008), North America (Kurt-Karakus et al., 2006), and India (Chakraborty et al., 2015). Modeling results have suggested that large parts of the global ocean have been losing dichlorodiphenyltrichloroethane (DDT) via volatilization (Stemmler and Lammel, 2009). In addition, air-sea exchange of PAHs has revealed that the seawater in the Mediterranean has turned into a temporary secondary source of PAHs, which is related to biomass burning in that region (Mulder et al., 2014). Moreover, melting ice and glaciers also have released OPs back into the atmosphere, which buffers the decline of OP levels in the polar regions (Ma et al., 2011; Geisz et al., 2008).

Similar to the polar regions, the Tibetan Plateau (TP) has been regarded as a "convergence" of OPs (Wang et al., 2016). Due to the continuous use of OPs in the surrounding countries and the "cold trapping" by the TP, the enrichment of OPs in the TP environment has been reported (Sheng et al., 2013; Wang et al., 2015). However, the TP has experienced great warming (Liu and Chen, 2000), and results of the air-soil exchange of OPs have indicated that the Tibetan soils are acting as a sink of DDT and higher molecular weight PAHs, but are a potential secondary source for hexachlorobenzene (HCB) and hexachlorocyclohexanes (HCHs) (Wang et al., 2014; Wang et al., 2012). This shows that the cold temperature over the TP might not be sufficient to trap volatile OPs. More studies on the air-surface exchange of OPs over

74 the TP are therefore needed to test the role of the terrestrial and aquatic ecosystems of

75 the TP in the regional cycling of OPs.

76 Known as "Asia's water power", the TP contains the headwaters of many major rivers

77 in Asia, which provide water sources for about one-sixth of the world's population

78 (Yao et al., 2012). The TP also has large numbers of remote lakes that are important

79 components of water bodies. Low temperature, oligotrophic conditions, and the long

80 duration of ice-cover are distinct features of these lakes. Based on the higher

81 atmospheric concentrations of α-HCH in summer, Xiao et al. (2010) deduced that

82 these enhanced concentrations may be caused by the thawing of lake ice, which

83 promotes the re-evaporation of α-HCH. However, the study did not include

84 measurements of HCH levels in lake water or the corresponding air-water exchange

85 analysis (Xiao et al., 2010). Therefore, it is still unclear whether the lake water of the

86 TP is the secondary source of a large number of OPs. Furthermore, biomass burning is

87 a widespread activity over the TP (Hu et al., 2015). A recent study demonstrated that

88 the locally sourced biomass combustion particles contributed substantially to the

89 black carbon (BC) loading of the TP glacier (Li et al., 2016). Given that PAHs and BC

90 both mainly originate from incomplete combustion of biomass, regional air-water

91 exchange of PAHs would also contribute to the overall air-surface exchange of

92 carbon.

93 We therefore conducted air and water sampling in a remote lake on the TP, and

94 assessed the air-water gas exchange, and the dry and wet deposition processes of

95 OCPs, PCBs, and PAHs. The aims of this study were to ascertain whether the Tibetan

96 lake represents a secondary source of OPs, to investigate the influence of seasonal

97 lake ice melting on the gas exchange of different OPs, and to estimate the contribution

98 of PAH exchange to the lake carbon budget.

2. Materials and methods

2.1 Site description

101 Nam Co Lake (30°30′–30°56′N, 90°16′–91°01′E, 4718 m) is located in the north of

102   the Nyainqentanglha Mountains, on the central TP (Figure 1). It is the second largest

103   lake in Tibet with an area of 2015 km^2 and a maximum depth exceeding 90 m (Wang

104   et al., 2009). The lake is mainly supplied by precipitation and glacier meltwater.

105   Annual riverine delivery of water to the lake is approximately 1.3×10^9 m^3 year^{-1},

106   while there is no outflow (Wu et al., 2014). The lake water is alkaline (pH=9.21) and

107   slightly saline (Wang et al., 2009). The climate of Nam Co is relatively cold and

108   windy with an annual average temperature of ~0 ℃ and an annual wind speed of ~4

109   m/s. The regional climate also has large seasonal variation: the Indian Monsoon

110   dominates summer (May to September) and the westerlies control winter climate

111   (October to April) [see the Supplement (S), Figure S1]. High temperatures and

112   precipitation are usually observed in summer (Figure S2), and the lake begins to thaw

113   from the beginning of May and melts completely by the end of May, which coincides

114   with the onset of the Indian Monsoon. During the winter, the lake is covered by ice

115   due to the subzero temperatures (Figure S2) and maximum instantaneous wind speeds

116   reaching up to 9.9 m/s.

117   The dominant land cover in Nam Co is alpine steppe and meadow, and the local

118   residents herd yak and sheep that graze around the lake. Biomass burning occurs for

119   heating, cooking, transport, and religious reasons. Near the southeastern shore, the

120   Nam Co Monitoring and Research Station for Multisphere Interactions (NCMORS) is

121   operated by the Chinese Academy of Sciences (Figure 1b). This station not only

122   facilitates the consecutive collection of field samples used in the current study, but

123   also provides local meteorological parameters for flux calculations.

124   **2.2 Air and water sampling**

125   An active air sampler (AAS) was deployed on the roof of NCMORS (Figure 1b) and

126   the air monitoring was conducted for two consecutive years from September 2012 to

127   September 2014. The flow rate of AAS was 60 L min^{-1} and the air samples were

128   collected every 2 weeks with a volume of approximately 600 m^3 for each sample. The

129   air stream passes first through glass fiber filters (GFFs 0.45 μm, Whatman) to collect

130   the total suspended particles (TSP) and then through polyurethane foam (PUF, 7.5×6

131 cm diameter) to retain the OPs in gas phase. In total, 47 air samples were collected.

132 Details regarding the sampling period, average air temperature, and wind speed are

133 given in Table S1. All harvested PUF and GFFs were stored at -20 ℃ until extraction.

134 To determine the OP levels in water, two sampling programs were conducted. First,

135 15 sites around the Nam Co Lake (surface lake water, 0–1 m depth) were selected to

136 obtain the spatial distribution of OPs in lake water (Figure 1b), which provides a

137 direct over-view of OP contamination over the lake. Second, monthly water samples

138 were collected at a site close to NCMORS (Figure 1b) from May to September, 2014

139 (water samples were not obtained during winter due to the ice cover). This provided

140 information regarding temporal variations in OP levels, isomer ratios, and the

141 enantiomeric fraction in lake water. Furthermore, coupled with the monthly average

142 air concentrations of individual OPs obtained, this allowed us to investigate the

143 air-water gas exchange of OPs (direction, flux, and monthly variations).

144 Water samples (200 L) were filtered with GFFs (0.7 μm, Whatman) to obtain the total

145 suspended particulate matter (SPM), and then pumped through an XAD-2 resin

146 column to collect the dissolved phase compounds. For each sampling month, triplicate

147 samples were collected. In total, 15 samples for the spatial study and 15 samples for

148 the temporal study were collected. XAD columns were kept at 4 ℃ until extraction.

149 The lake water properties (temperature, pH and salinity) are provided in Table S2.

150 **2.3 Sample extraction and analysis**

151 The chemical extraction and cleanup methods are detailed in Text S1 for each sample

152 type [air (PUF plug), TSP, water (XAD column), and SPM]. OPs were analyzed on a

153 gas chromatograph with an ion-trap mass spectrometer (GC-MS, Finnigan Trace

154 GC/PolarisQ) operating under MS–MS mode. More information on the

155 chromatographic conditions is given in Text S2. The target compounds are as follows:

156 HCHs (including α-HCH, β-HCH, and γ-HCH), HCB, DDTs (o,p'-DDE, p,p'-DDE,

157 o,p'-DDT, and p,p'-DDT), PCBs (PCB 28, PCB 52, PCB 101, PCB 138, PCB 153,

158 and PCB 180), and 15 priority PAHs listed by the United States Environment

159   Protection Agency (USEPA, without naphthalene), including acenaphthylene (Acel),

160   acenaphthene (Ace), fluorene (Flu), phenanthrene (Phe), anthracene (Ant),

161   fluoranthene (Fla), pyrene (Pyr), benz[a]anthracene (BaA), chrysene (Chr),

162   benzo[b]fluoranthene (Bbf), benzo[k]fluoranthene (Bkf), benzo[a]pyrene (BaP),

163   dibenz[a, h]anthracene (DahA), benzo[g, h, i]perylene (BghiP), and

164   indeno[1,2,3-cd]pyrene (IcdP). Enantiomers of α-HCH were determined with a

165   BGB-172 chiral column (see Text S2 for details). The chiral signature of α-HCH is

166   expressed using the enantiomeric fraction (EF), which is equal to the ratio of peak

167   areas of the (+)/[(+) + (−)] (Harner et al., 2000).

2.4 Quality assurance/quality control (QA/QC)

169   All analytical procedures were monitored using strict QA/QC measures. Prior to

170   sampling, PUF and XAD resin were pre-cleaned using dichloromethane (DCM) for

171   16 h and GFFs were baked at 450 ℃ for 4 h. Six PUF field blanks, three XAD field

172   blanks, and six procedural blanks were prepared; HCB, Phe, Ant, Fla, and Pyr were

173   detected in the field blanks (Table S3). The definitions of the method detection limits

174   (MDLs) are described in Text S3, and the derived MDLs are given in Table S4. The

175   breakthrough of PUF plugs was checked in eleven split PUFs, and the results show

176   that the individual OPs in the second half varied from 8% to 23% (Table S5),

177   indicating good retention capacity. Certified surrogate standards (from Dr.

178   Ehrenstorfer GmbH, Germany) were added to each sample before extraction and

179   analysis. The recoveries ranged from 71% to 94% for PCB 30, 79% to 105% for

180   Mirex, and 65% to 92% for perylene-D12. The reported concentrations were

181   subtracted by mean blanks but not corrected for recoveries. To check the

182   reproducibility of the chiral analysis, the racemic standard of α-HCH was injected

183   repeatedly and its average EF value was 0.499 ± 0.001 (n = 5).

2.5 Calculations of air-water gas exchange

185   Concurrent air and water samples were used to assess the status of air-water gas

186   exchange in Nam Co Lake. The gas exchange direction can be determined by the ratio

187   of fugacity in water (f_w) and air (f_a), giving the fugacity ratio (f_w/f_a) (Jantunen et al.,

188   2015):

$$f_a = C_G R T_a \tag{1}$$

$$f_w = C_w H \tag{2}$$

191   where C_G and C_w are the gaseous and dissolved concentrations of target compounds in

192   air and water (mol m^{-3}), respectively, R is the gas constant (8.314 Pa m^3 mol^{-1} K^{-1}), T_a

193   (K) is the air temperature, and H (Pa m^3 mol^{-1}) is the Henry's law constant. Due to the

194   possible sorption by dissolved organic carbon (DOC), OPs retained by XAD were

195   DOC-corrected to derive the truly freely dissolved concentrations in water (Text S4)

196   (Gonzalez-Gaya et al., 2016). H values were adjusted for the real water temperature

197   and salinity of Nam Co by the procedure described in Text S5 (Cetin et al., 2006; Ma

198   et al., 2010). The uncertainty involved in f_w/f_a was estimated by propagating the errors

199   in C_a (30%), C_w (35%), and H (20%), which was 50%. Accordingly, ratios of f_w/f_a

200   between 0.5 and 1.5 are assumed as air-water equilibrium, while $f_w/f_a > 1.5$ and <0.5

201   indicate net volatilization and deposition, respectively.

202   Net fluxes of air-water gas exchange (F_{AW}, ng m^{-2} day^{-1}) were quantified using the

203   Whitman two-film model, which has been used in many previous studies (Iwata et al.,

204   1993; Khairy et al., 2014):

$$F_{AW} = K_{ol}\left(C_w - C_G R T_a / H\right) \tag{3}$$

206   where K_{ol} (m s^{-1}) is the overall mass transfer coefficient, which contains contributions

207   from the mass transfer coefficients of the water and air layers, K_w and K_a, respectively.

208   They are related to the wind speed and compound-specific molecular diffusivity; a

209   detailed calculation is presented in Text S6. Positive flux values indicate net

210   volatilization, and negative values indicate net deposition.

211   **2.6 Estimation of dry and wet deposition fluxes**

212   In addition to the gas exchange, dry and wet deposition are also important processes

213   that control the input of OPs from air to lake. Dry deposition fluxes (F_{DD}, ng m^{-2} day^{-1})

214   of atmospheric particulate-phase OPs can be calculated using (Gonzalez-Gaya et al.,

215   2016) the following equation:

216 $F_{DD}=0.864V_D C_P$ (4)

217   where V_D (cm s^{-1}) is the compound specific deposition velocity, C_P is the measured

218   OPs concentrations in TSP (pg m^{-3}), and 0.864 is a unit conversion factor. V_D for each

219   sampling period and compound was estimated using an empirical equation derived by

220   Gonzalez-Gaya et al. (2014):

221                          $\log(V_D)=-0.261\log(P_L)+0.387U_{10}Chl_s-3.082$ (5)

222   where P_L (Pa) is subcooled liquid vapor pressure of chemicals that was corrected to

223   the local temperature using the equations given in Table S6, U_{10} (m s^{-1}) is wind speed

224   at 10 m height converted from the field-measured wind speed at 1.5 m (Table S1), and

225   Chls is the surface chlorophyll concentration (mg m^{-3}, Liu et al., 2010).

226   Wet deposition fluxes by rain (F_{WD}, ng m^{-2} day^{-1}) were estimated using the method

227   established by Jurado et al. (2005):

228                                  $F_{WD}= P(W_G C_G + W_P C_P)$ (6)

229   where P is precipitation depth per day (m d^{-1}) derived from the data recorded in the

230   NCMORS, and W_G and W_P are the gas and particle washout ratios, respectively.

231   Assuming that equilibrium is attained between the gas phase and the dissolved phase

232   in a raindrop, W_G was estimated by (Wania et al., 1998a):

233 $W_G=RT_a/H$ (7)

234   The recommended value of W_P in Jurado et al. (2005) was used to consider the

235   particle scavenging by rain.

236   For snow deposition, the fluxes were calculated by adopting the washout ratios

237   reported in Franz and Eisenreich (1998) (Table S7).

3. Results and discussion

239   We determined the OP concentrations in air, TSP, water, and SPM separately; the full

240   data sets are listed in Tables S8-S11. OCPs and PCBs were rarely detected in TSP

241   (Table S9), and were therefore not considered in further discussion. Comparisons

242   between the data from this study and previously published values for the TP and other

243   remote regions are presented in Tables S12-S15.

3.1 Levels of OPs in air and water at Nam Co

The concentrations of OPs in the atmosphere and TSP in Nam Co are summarized in Figure 2 using box-and-whisker plots. Among the OCPs, HCB was the dominant chemical with an average concentration of 20 pg m^{-3} (Figure 2a), which was two times higher than that reported for southeastern TP (Sheng et al., 2013) and Mt. Everest (Li et al., 2006) (Table S12), but lower than the values in the Rocky Mountains (42 pg m^{-3}, Wilkinson et al., 2005) and the Arctic (64 pg m^{-3}, Su et al., 2006). The α-HCH (average 4.0 pg m^{-3}) and γ-HCH (2.1 pg m^{-3}) values in this study were much lower than those measured using a flow-through sampler (FTS) during 2006 to 2008 (48.7 and 7.9 pg m^{-3}, respectively) (Xiao et al., 2010). The DDT concentrations in the current study (0.8-46.4 pg m^{-3}) were lower than those observed for Lulang in southeastern TP (Table S12) (Sheng et al., 2013), which is the entrance of the Indian Monsoon. In spite of this, the levels of DDTs were still one order of magnitude higher than those for the Arctic (Table S12) (Su et al., 2008). Lower concentrations of $\sum_6$PCBs were also detected in air with an average value of 2.5 pg m^{-3}.

The sum concentrations of $\sum_{15}$PAHs in the atmosphere ranged from 0.5–13 and 0.1–3.4 ng m^{-3} in the gaseous and particulate phases, with averages of 2.2 and 0.6 ng m^{-3}, respectively. The 3- and 4-ring PAHs were predominant in both phases, including Phe, Flu, Fla, and Pyr (Figure 2b and 2c). The PAH levels in Nam Co were one order of magnitude lower than those reported for Lhasa (35.7 ng m^{-3}, Table S13), which is the capital city of Tibet with a large population, extensive tourism, and abundant religious activities (Gong et al., 2011). Compared with background levels in other regions of the world (Table S13), the PAHs in this study were comparable to the levels in Arctic air (Ding et al., 2007), but significantly higher than those from European mountainous regions (Fernandez et al., 2002).

In the lake water, the average dissolved concentrations of α-HCH, β-HCH, γ-HCH, HCB, and PCB 28 were 9.9, 85.2, 7.0, 7.6, and 1.9 pg L^{-1}, respectively; while DDT-related compounds were below MDLs in most cases for both dissolved and

273 SPM phases (Table S10 and S11). The current measured HCH concentrations were

274 approximately two orders of magnitude lower than values reported for the Yamdrok

275 and Co Ngoin Lake in 2002 (Table S14) (Zhang et al., 2003). Two possible reasons

276 for this discrepancy are: i) the inter-annual variation of chemicals, i.e., the

277 concentrations declined rapidly since 2002; and ii) the uncertainties caused by

278 analytical and instrumental method (electron capture detector in Zhang et al. (2003)

279 study and the MS detector in the current study). From a global perspective, the HCH

280 concentrations obtained by this study were overall lower than those in European

281 mountain lakes (Table S14). DDT class chemicals were rarely detected and only PCB

282 28 could be quantified in the Nam Co lake water. These features combined with the

283 low levels of HCHs suggest that the OP levels in Nam Co lake water were close to the

284 values reported for ocean waters, such as, the North Atlantic and Arctic oceans (with

285 DDTs and PCBs mostly below the detection level, or <1 pg L^{-1}) (Gioia et al., 2008;

286 Lohmann et al., 2009). By contrast, high levels of PAHs were found in the Nam Co

287 lake water, ranging from 6.9 to 83.6 and 1.7 to 28 ng L^{-1} for the dissolved and SPM

288 phases, respectively. The dissolved $\sum_{15}$PAH levels were one order of magnitude

289 higher than those reported for Himalayan high-altitude lakes in Nepal (Table S15)

290 (Guzzella et al., 2011) and the Great Lakes (Table S15) (Venier et al., 2014), and two

291 orders of magnitude greater than values for open oceans (Table S15) (Ma et al., 2013)

292 and European mountain lakes (Table S15) (Vilanova et al., 2001).

293 **3.2 Possible sources**

294 Long range atmospheric transport (LRAT) is considered an important source

295 contributing to the occurrence of OPs in remote environments (Dalla Valle et al.,

296 2005). Considering that the prevailing climate system operating over Nam Co in

297 summer is the Indian Monsoon, if the seasonal pattern of a chemical is similar to that

298 of the monsoon, monsoon transport may therefore be the source of OPs in Nam Co air.

299 Thus, the interrelationship between monsoon intensity (Indian Monsoon Index, IMI,

300 W m^{-2}) and OP concentrations was investigated (Figure 3). Figure 3 shows that

301 α-HCH and *o,p'*-DDT displayed synchronous seasonal variation with the IMI. This

302   suggests that monsoon transport was the principal reason for the occurrence of OCPs

303   in the Nam Co atmosphere. In addition, isomer ratios can provide insight on the

304   source and fate of the OPs. In this study, we found that the isomer ratios of *p,p'*-DDT

305   to *p,p'*-DDE were broadly in agreement with those found for the source regions of

306   India and the Bay of Bengal (Table S16) (Gioia et al., 2012; Zhang et al., 2008).

307   Similar to other remote regions, such as, the Arctic (Hung et al., 2010), Antarctic

308   (Baek et al., 2011), Rocky Mountains (Daly et al., 2007), and southeastern TP (Sheng

309   et al., 2013), in which LRAT is the primary transport mode of OPs, the dominance of

310   α- to γ-HCH was observed in the Nam Co atmosphere (Table S16). Results of isomer

311   ratios associated with the seasonal variations supported the interpretation that OCPs in

312   the Nam Co atmosphere had undergone LRAT. In contrast to OCPs, neither the

313   gaseous nor the particulate phases of PAHs showed a clear and consistent seasonal

314   variation during the two years of air monitoring (Figure S3), which is likely because

315   there were primary emissions of PAHs surrounding the Nam Co region.

316   Apart from the seasonal trends, spatial distribution patterns can also provide valuable

317   information on OP sources. The spatial distributions of OPs in the surface water

318   across the Nam Co Lake are presented in Figure 4. First, HCHs showed a uniform

319   distribution (Figure 4a) without significant differences among the different regions of

320   the lake (Table S17). The even distribution of HCHs in the water was most likely

321   caused by the LRAT origins and relatively higher water solubility. Second, relatively

322   high levels of HCB and PAHs occurred in water from the northwestern and eastern

323   parts of the lake (Table S17, Figure 4b and 4c). The elevated HCB and PAHs in these

324   regions were likely related to anthropogenic activity in the vicinity. As shown in

325   Figure 1b, two townships (Baoji and Namco), which have the highest population

326   around Nam Co Lake, are located in the northwestern and eastern corners of the lake.

327   Following a traditional lifestyle, the residents use large amounts of local biomass

328   (mostly yak dung) for cooking and heating (Xiao et al., 2015). High PAH

329   concentrations have been reported in local Tibetan tents that were emitted mainly

330   from burning yak dung (Li et al., 2012). A ratio of BaA/(BaA+Chr) = 0.33 was

331 recommended as a specific diagnostic fingerprint for yak dung combustion (Li et al.,

332 2012). The BaA/(BaA+Chr) ratios observed in our study (0.27±0.08 for air and

333 0.24±0.10 for water) were in good agreement with this diagnostic ratio. This suggests

334 that local combustion emission is likely the source of PAHs in Nam Co. With the

335 exception of PAHs, biomass combustion can also produce HCB (Bailey, 2001), which

336 may be the reason for the higher HCB concentrations occurring around the townships.

337 The spatial distribution of OPs in the Nam Co lake water highlights the important

338 contribution of local sources for PAHs and HCB.

3.3 LRAT versus re-volatilization

340 From the above results, we found that LRAT is a key factor that determines the

341 seasonality of the atmospheric HCHs and DDTs in Nam Co (higher concentrations

342 occurred in summer). However, high temperatures generally occur during summer,

343 which may promote the evaporation of chemicals from local surfaces (e.g., soils and

344 water bodies). To what extent does this re-evaporation contribute to the atmospheric

345 OPs? The Clausius-Clapeyron (C.C.) equation can be used to assess this probability

346 (Wania et al., 1998b). If a strong relationship is found between the partial pressure of

347 atmospheric OCPs and the air temperature, this indicates that volatilization may occur.

348 Otherwise, low temperature dependence will occur in the case of LRAT. In the

349 present study, the results of the C.C. equation are summarized in Table S18. The

350 correlation with temperature ($p>0.05$, Table S18) for most chemicals was not

351 significant, except for α-HCH, which displayed a relatively lower correlation

352 coefficient ($R^2=0.29$, $p<0.05$, Table S18). This indicates that weak volatilization of

353 α-HCH from local surfaces at Nam Co may exist, while the re-evaporation of other

354 chemicals is limited.

355 Enantiomers of chiral OPs have been used to distinguish the contribution of LRAT

356 and re-volatilization of OPs from surfaces (Bidleman et al., 2012). For example,

357 technical HCH contains the (+)- and (-)-α-HCH enantiomers in a racemic proportion

358 (EF=0.5). Abiotic processes (transport, hydrolysis, and photolysis) do not favor either

359 enantiomer, while only biological processes, such as, microbial degradation in soils

360   and water, show enantioselectivity and will alter the EFs of α-HCH (Ridal et al.,

361   1997). Therefore, nearly racemic signatures usually indicate input from LRAT, while

362   nonracemic signatures represent the influence of local microbial degradation. In the

363   present study, both the enantiomeric signatures of α-HCH in air and water were

364   measured simultaneously from May to September. As shown in Figure 5a, all the lake

365   water samples showed a selective depletion of (+)-α-HCH, with EFs ranging from

366   0.318 to 0.449. This has previously been reported for other cold oligotrophic water

367   systems, such as the Arctic lakes (EFs: 0.359−0.432) (Law et al., 2001). From Figure

368   5a, we found that extensive enantioselective degradation occurred in June and July,

369   which coincided with the bacterial bloom period (Figure 5b) (Liu et al., 2013). This

370   negative correlation between the EF of α-HCH in lake water and bacterial abundance

371   is presented in Figure S4. Law et al. (2001) suggested that under low nutrient

372   conditions, oligotrophic bacteria are able to use xenobiotic carbon sources, such as

373   α-HCH. This implies that the Tibetan lake microbes can also metabolize, or

374   cometabolize, α-HCH.

375   If high temperatures favor the evaporation of α-HCH from the lake water, depletion of

376   (+)-α-HCH should be observed for air. However, the EFs of the air samples were

377   overall racemic. This is similar to the racemic composition observed in the

378   atmosphere over Indian regions (Huang et al., 2013), which is the potential source

379   region of HCHs in Nam Co. With respect to the enantiomeric signature in air samples

380   from June and July, only some (+) α-HCH depletion was observed in air (Figure 5a),

381   indicating weak evaporation of α-HCH from the lake water. Combined with the EF

382   values in air and water, the fraction of the contribution from lake water volatilization

383   (*f*) can be quantified by (Huang et al., 2013):

384   $$f = \left(EF_a\text{-}EF_b\right)/\left(EF_w\text{-}EF_b\right) \tag{8}$$

385   where EF_a and EF_w are the EF values in air and water, respectively; and EF_b is the

386   background EF value in air, which was assumed to be the average EF of the standard.

387   The estimated results show that only 19% and 17% of atmospheric α-HCH came from

388   water volatilization in June and July, respectively, demonstrating that LRAT is indeed

389 the major source (more than 80%) of α-HCH. This result is in contrast with the

390 conclusion of Xiao et al. (2010) that evaporation from Nam Co Lake largely

391 contributed to the atmospheric α-HCH concentration. In that study, both levels and

392 enantiomeric signatures of α-HCH in Nam Co lake water were absent.

393 **3.4 Atmospheric processes**

394 **3.4.1 Air-water gas exchange**

395 Although some α-HCH evaporation was recorded in June and July, the air-water

396 exchange process during the entire ablation period is of great concern as this is the

397 main season transferring pollutants between air and water. Fugacity ratios (f_w/f_a) and

398 net exchange fluxes (F_{AW}, ng m^{-2} day^{-1}) were quantified using paired air-water

399 samples collected from May to September in 2014. The average exchange status

400 (average of f_w/f_a) for HCHs, HCB, PCB 28, and PAHs during the ablation period is

401 illustrated in Figure 6. Because of DDTs, Ant and Fla were not quantified in the lake

402 water (Table S10) and were therefore excluded from the discussion. α- and γ-HCH

403 had low f_w/f_a values ranging from 0.08 to 0.15, and 0.02 to 0.08, respectively (Figure

404 6a). The low f_w/f_a ratio suggests that α- and γ-HCH were overall prone to deposition

405 from air to water during the ablation period. The deposition fluxes were -1.6 ± 0.4 ng

406 m^{-2} day^{-1} for α-HCH and -1.0 ± 0.2 ng m^{-2} day^{-1} for γ-HCH, which are within the

407 same order of magnitude as those reported for the Great Lakes (Khairy et al., 2014).

408 Connected to the source of HCHs discussed above, this result implies that the

409 following LRAT-deposition event of HCHs occurred in the ablation period of Nam Co

410 Lake. In terms of β-HCH, HCB, and PCB 28, their f_w/f_a ratios were either overlapping

411 with the equilibrium range (0.5-1.5) or on the edge of deposition threshold. Therefore,

412 low deposition fluxes for β-HCH (-0.2 ng m^{-2} day^{-1}) and PCB 28 (-0.1 ng m^{-2} day^{-1}),

413 and large variability for HCB (-1.0 ± 0.6 ng m^{-2} day^{-1}) were observed (Figure 7a).

414 The results of the air-water gas exchange for PAHs are presented in Figure 6b. The

415 fugacity ratios of thirteen PAHs varied depending on their molecular weight and

416 volatility (Figure 6b). Acel, Ace, and Flu showed f_w/f_a values significantly higher than

417 1.5 (Figure 6b), indicating that the lake acted as a secondary source for these volatile

418 chemicals. The f_w/f_a values for Phe covered a large range (from 0.3 to 3), showing a

419 shift between volatilization and deposition (Figure 6b). Other high molecular weight

420 (MW > 202) PAHs, including Pyr, BaA, Chr, Bbf, Bkf, Bap, IcdP, DahA, and BghiP,

421 favored net deposition with f_w/f_a values lower than 0.5 (Figure 6b). Greater

422 volatilization fluxes were observed for Acel, Ace, and Flu (3-ring), which could reach

423 up to 203 ng m^{-2} day^{-1} (Figure 7b). Whereas, the gaseous deposition fluxes for high

424 molecular weight PAHs were two orders of magnitudes lower and only varied from

425 -1.0 to -4.6 ng m^{-2} day^{-1} (Figure 7c). Although average deposition fluxes of 339 ng

426 m^{-2} day^{-1} were calculated for Phe, the deposition fluxes showed large variability (± 604

427 ng m^{-2} day^{-1}). This result is broadly consistent with the exchange direction revealed by

428 the f_w/f_a values, implying that the exchange of Phe between air and water may be

429 reversed during the entire ablation period.

430 **3.4.2 Reversal of the air-water exchange of Phe**

431 In section 3.4.1, we observed that both the air-water exchange direction and the flux

432 of Phe showed a large range of values and uncertainties. This raises a question about

433 what drives this variation. The monthly calculated f_w/f_a and F_{AW} of Phe during the

434 ablation period showed that the volatilization of Phe occurred during May and June,

435 but deposition begun in July, which represents a reversal (Figure 8). Given that lake

436 ice begins melting during May, the melted ice may discharge large amounts of

437 accumulated PAHs into the lake, causing the relative enrichment (high fugacity) of

438 Phe in the water, and triggering the secondary emission of Phe from the water to the

439 atmosphere. This was confirmed by the increased water concentration of Phe found

440 during May and June (Table S10). This is also the reason why a large uncertainty of

441 F_{AW} was observed for Phe during the ablation period. Linked to the source of PAHs

442 discussed above, the final exchange status of PAHs is the combined effects of the

443 depositional input caused by biomass burning, the properties of the chemical, and the

444 melting of lake ice.

445 Seasonal ice cover is an important feature of water bodies in cold regions. In the

446 Arctic region, Jantunen et al. (2008) and Wong et al. (2011) both observed the

447 occurrence of volatilization of OCPs from seawater coincident with the breaking up of

448 ice cover in the summer. The Nam Co Lake also undergoes long periods of ice-cover

449 (Liu et al., 2013). During the winter, the lake surface is covered by ice and gas

450 exchange is restricted, meanwhile dry and wet deposition exerts a significant

451 influence on the input inventory of PAHs to the lake. Both of these two deposition

452 processes are one-way (no volatilization), which keeps the contaminants being

453 accumulated. As summer arrives, the lake ice begins to thaw and air-water gas

454 exchange begins to dominate. On the one hand, after the higher accumulation of

455 deposition, supersaturation of PAHs in the lake may occur. On the other hand, the

456 fugacity capacity of ice is much higher than that of water, and therefore the decrease

457 of the fugacity capacity during melting will increase the fugacity of the PAHs (Wania

458 et al., 1998c), which also promotes their re-emission from the water. Although the

459 seasonal ice cover did not show any obvious influence on the fate of OCPs and other

460 PAHs, it played an important role in the fate of Phe, which was a dominant compound

461 in the Nam Co atmosphere. The lake therefore acted as a secondary source of Phe in

462 May and June, and shifted to a net sink during other months, which is likely driven by

463 the seasonal freeze-thaw cycle of lake ice (Figure 8).

464 **3.4.3 Atmospheric degradation**

465 Reactions with the hydroxyl radical (OH) are an important removal process of

466 gaseous OPs from the atmosphere. The resulting degradation fluxes (F_{deg}, ng m^{-2} day^{-1})

467 are dependent on the concentration of OH radicals in the air (Spivakovsky et al., 2000)

468 and the compound-specific degradation rate constant (K_{OH}, cm^3 molecules^{-1} day^{-1}).

469 The K_{OH} values of gaseous OCPs and PAHs are from Brubaker and Hites (1998) and

470 Keyte et al. (2013), respectively. Due to the lack of information on K_{OH} for β-HCH

471 and BaA, their degradation fluxes (F_{deg}) were not considered in this study. The

472 calculated F_{deg} values were averaged for individual OPs and are presented in Figure

473 S5. The degradation fluxes for α-, γ-HCH, HCB, and PCB 28 ranged between 0.3 and

474 0.9 pg m^{-2} day^{-1} (Figure S5), 3 orders of magnitude lower than their F_{AW}. This

475 indicates that the contribution of atmospheric degradation to their total inventory in

476   the environment is negligible.

477   In contrast to the OCPs, the PAHs are more susceptible to photodegradation

478   (Lohmann et al., 2009). In our study, lower molecular weight PAHs showed higher

479   degradation fluxes, such as 4–184 ng m^{-2} day^{-1} for Phe, and 1–160 ng m^{-2} day^{-1} for

480   Ant (Figure S5). These values are similar to those reported for F_{deg} in the remote

481   atmosphere of the Atlantic Ocean (i.e., 7–120 and 9–50 ng m^{-2} day^{-1} for Phe and Ant,

482   respectively) (Nizzetto et al., 2008). We observed relatively low F_{deg} values for 5- and

483   6-ring PAHs, ranging from 0.01 to 0.18 ng m^{-2} day^{-1} (Figure S5). Generally, the F_{deg}

484   of all PAH compounds was one order of magnitude lower than their F_{AW}. OH

485   depletion is the primary process that removes atmospheric PAHs, presumably causing

486   the continuous volatilization of low molecular weight PAHs from the water. This

487   raised questions about other processes that may have supplied PAHs into the lake

488   water. On the other hand, OH degradation also decreases the input of high molecular

489   weight PAHs into the water and it is unclear to what extent this degradation

490   counteracts other deposition processes.

491   **3.4.4 Atmospheric deposition**

492   In addition to the gas exchange, dry and wet deposition are also important processes

493   that influence the input of OPs from air to the lake. Dry (F_{DD}) and wet (F_{WD})

494   deposition fluxes were estimated using the method described above (section 2.6).

495   With respect to HCHs, HCB, and PCB 28, their dry deposition fluxes (F_{DD}) were

496   negligible due to their low detection frequency in the particulate phase (Table S9).

497   However, the average F_{WD} for α-HCH, β-HCH, and γ-HCH was -0.3, -0.9, and -0.4 ng

498   m^{-2} day^{-1}, respectively, which is comparable to their F_{AW} levels. F_{WD} for HCB (-0.02

499   ng m^{-2} day^{-1}) and PCB 28 (-0.002 ng m^{-2} day^{-1}) was two magnitudes lower than their

500   F_{AW}. In general, precipitation scavenging is most efficient in HCHs compared with

501   the other chemicals (Carrera et al., 2002). Greater wet deposition fluxes of HCHs

502   occurred in August (Figure S6), coinciding with the highest amount of precipitation in

503   Nam Co. Combining the F_{AW} and F_{WD} of HCHs, the estimated annual input of HCHs

504   from air into the whole lake (2015 km^2) was 1.9 kg year^{-1}. This result highlights the

505   input of HCHs by the LRAT-deposition process during the ablation period (open

506   water season). Snow scavenging of HCHs has been reported as an important clearing

507   process in mountain regions (Kang et al., 2009). However, the transport of HCHs in

508   winter is very limited due to the unfavorable air circulation patterns (westerly wind),

509   ruling out the significant contribution of input of HCHs by snow scavenging.

510   Compared with OCPs, the close association between PAHs and the particulate phase

511   accounted for their relatively higher deposition fluxes. The estimated dry and wet

512   deposition fluxes for individual PAHs during the ablation and frozen periods,

513   respectively, are provided in Table 1. We found that the F_{DD} values of PAHs for the

514   ablation period are, in general, lower than those for the frozen period. For example,

515   the F_{DD} of total $\sum_{15}$PAHs increased by one order of magnitude from the ablation

516   period (4.5 ng m^{-2} day^{-1}) to the frozen period (38 ng m^{-2} day^{-1}; Table 1). Two factors

517   may lead to the increase of F_{DD} in winter: the increased wind speed during the winter

518   season and the growing particulate-PAH concentrations due to the enhanced

519   combustion activities in winter. Compared with other studies, the estimated F_{DD} for

520   the total $\sum_{15}$PAHs (4.5–38 ng m^{-2} day^{-1}, this study) is broadly within the range

521   reported for global oceans (8.3–52.4 ng m^{-2} day^{-1}) (Gonzalez-Gaya et al., 2014).

522   Wet deposition was found to be the dominant deposition process for the input of PAHs

523   into Nam Co (Table 1). This was expected because precipitation scavenging of

524   organic chemicals underlies the accumulation of pollutants in mountain regions

525   (Tremolada et al., 2008). In addition, there was an obvious difference between the

526   values of F_{WD} during the ablation and frozen periods. For the total 15 PAHs, the F_{WD}

527   in the frozen period (702 ng m^{-2} day^{-1}) was approximately 5 times higher than that for

528   the ablation period (161 ng m^{-2} day^{-1}), which may be due to the different precipitation

529   types between these two periods (snow *vs.* rain). Snow has been suggested to be more

530   efficient than rain for scavenging particulate-PAHs, which had a high concentration

531   during winter in Nam Co (Table S9). Thus, although the precipitation of Nam Co in

532   winter is low (less than 30 mm, Figure S2), the strong scavenging ratio of snow to

533   PAHs combined with the relatively high particulate-PAHs concentration in winter

534   caused the enhanced PAHs deposition in winter. The frozen season coincided with the

535   period of high emission and high deposition of PAHs, implying a significant

536   contribution of this season in the input of PAHs into the lake.

537   To calculate the comprehensive contribution of all above-mentioned processes, three

538   groups of PAHs were classified in Table 1 based on their fate during the air-water

539   exchange processes. PAHs (Acel, Ace, and Flu) showing volatilization behavior were

540   placed into one group, PAHs with large F_{AW} variability between the status of

541   volatilization and deposition were in the second group; and the remaining PAHs

542   displaying deposition behavior were placed into the third group (Table 1). In this

543   classification, although the air-water exchange direction and fluxes of Ant and Fla

544   cannot be estimated, we still placed them into the second group because of their

545   similarity to Phe in their physicochemical properties. For the volatilization group, the

546   total outgassing from the lake was estimated to be approximately 126 kg per year,

547   which cannot alone be supplied by their total deposition flux (sum of F_{WD} and F_{DD}).

548   This suggests that there may be additional natural sources of PAHs in the lake, such as,

549   degradation of pigments carrying aromatic structure and turnover of organic matter

550   (Nizzetto et al., 2008). Regarding the deposition group (Pyr, BaA, Chr, Bbf, Bkf, Bap,

551   IcdP, DahA, and BghiP), their total deposition flux ($F_{AW}+F_{DD}+F_{WD}$) will roughly

552   cause the annual input of 208 kg high molecular weight PAHs into the lake. Although

553   the F_{AW} of Phe was reversed and the total volatilization of Phe was estimated at

554   around 26 kg year^{-1}, this loss will be complemented by the continuous deposition of

555   Phe (~373 kg year^{-1}) from July to April. This indicates that the annual net input of Phe

556   will be above 340 kg, which suggests that Phe is the most dominant contributor in the

557   total PAHs deposition. In addition to the 15 PAHs considered here, there are other

558   PAHs with high abundances, for example alkylated phenanthrenes, which will drive a

559   much larger depositional fluxes to the lake.

560   **3.4.5 Uncertainties in flux estimation**

561   Several factors were involved in the uncertainties of the flux estimation: (i) loss

562   during sample extraction and clean-up; (ii) measurement errors; and (iii) accuracy of

563   the parameters in meteorology and physicochemical properties. The air-water gas

564   exchange flux (F_{AW}) is the most important contributor to the total inventory of PAHs

565   into the lake. The uncertainty involved in F_{AW} was estimated by propagating the

566   errors in C_a (30%), C_w (35%), K_{ol} (40%), and H (20%), which was 64%. This small

567   error demonstrates that the estimate of the gas exchange fluxes was relatively robust.

568   By contrast, the uncertainties in other fluxes were higher. The uncertainty of F_{DD} was

569   estimated as a factor of 3 (Gonzalez-Gaya et al., 2014). However, the uncertainties of

570   F_{deg} and F_{WD} are difficult to quantify due to unavailable data on the relative errors of

571   K_{OH}, W_G, and W_P. For example, the scavenging rates of PAHs by wet deposition were

572   highly variable, which was caused by the complexity of the size distribution of

573   aerosols, meteorological conditions, and the scavenging process (Jurado et al., 2005).

574   Considering these aggregated uncertainties, the estimated total fluxes here are only

575   expected to capture the order of magnitude for the different processes. In addition,

576   other input processes into the lake, such as, glacier meltwater, river runoff, and soil

577   erosion may also occur in this study region, which will lead to an underestimation of

578   the total input flux.

579   **3.5 Implication for the regional carbon cycling**

580   Lakes are increasingly recognized as an important component of the terrestrial carbon

581   cycle (Tranvik et al., 2009). Nearly 50% of the area of Chinese lakes is located on the

582   TP, with general oligotrophic conditions and a total lake area of >43000 km^2 (Zhang

583   et al., 2014). Compared with other components, such as grassland and forest, organic

584   carbon burial in Tibetan lakes has been largely ignored. Although our study only

585   focused on one of these lakes (Nam Co, area = 2015 km^2), we can extrapolate the

586   annual atmospheric deposition of $\sum_{15}$PAHs into the remaining Tibetan lakes, and

587   estimate it at 8.7 tonnes C, when expressed as carbon fluxes (Gonzalez-Gaya et al.,

588   2016). In addition to these 15 PAHs, there are other carbon sources such as soot, DOC,

589   PAHs derivatives, and other anthropogenic organic compounds, which would become

590   a significant allochthonous carbon source for the oligotrophic lakes in TP. Because the

591   Tibetan lakes are low in nutrients, bacteria in the lake have adapted to using a wide

range of organic compounds and growing under starvation conditions (Liu et al., 2009). Recently, bacteria from the genus *Sphingomonas* were detected in Nam Co lake water and various glacier snows of the TP (Liu et al., 2013; Liu et al., 2009), and they were reported to have the ability to degrade PAHs (Leys et al., 2005). The presence of these bacteria in Nam Co suggests that the atmospheric inputs of organic pollutants can act as a carbon source to support the survival of Tibetan microbial communities. Despite the natural PAH background in the environment, increasing biomass burning has led to the accumulation of PAHs in the lake sediments, especially during the past 50 years (Yang et al., 2016). Therefore, the continuous atmospheric deposition of various PAHs and their ecological impact deserve greater concern.

4. Conclusions

This study confirmed that the Nam Co Lake was still a net sink of HCHs, following the LRAT-deposition process, rather than a secondary source. By contrast, PAHs primarily originated from local biomass burning. Dominated by gas exchange and wet deposition, the air-water fluxes of $\sum_{15}$PAHs to the whole Nam Co Lake were estimated to be 550 kg year^{-1}, providing a substantial carbon source for the oligotrophic lake. Among the PAHs compounds, Phe showed a distinct behavior with monthly reversals of the air–water exchange, which was most likely driven by the seasonal melting of lake ice. This hypothesis requires further investigation, and a passive sampling technique is recommended as a viable alternative to enhance the spatial coverage of the investigation of air-water exchange in the TP.

Acknowledgments

This study was supported by the National Natural Science Foundation of China (41671480, 41222010 and 41571463) and Youth Innovation Promotion Association (CAS2011067). The authors would like to thank the staff at Nam Co Monitoring and Research Station for Multisphere Interactions for their help with the field sampling.

References:

Baek, S. Y., Choi, S. D., and Chang, Y. S.: Three-Year Atmospheric Monitoring of Organochlorine Pesticides and Polychlorinated Biphenyls in Polar Regions and the South Pacific, Environ. Sci. Technol., 45, 4475-4482, doi: 10.1021/Es1042996, 2011.

Bailey, R. E.: Global hexachlorobenzene emissions, Chemosphere, 43, 167-182, doi: 10.1016/S0045-6535(00)00186-7, 2001.

Bidleman, T. F., Jantunen, L. M., Kurt-Karakus, P. B., and Wong, F.: Chiral persistent organic pollutants as tracers of atmospheric sources and fate: review and prospects for investigating climate change influences, Atmospheric Pollution Research, 3, 371-382, doi: 10.5094/Apr.2012.043, 2012.

Brubaker, W. W., and Hites, R. A.: OH Reaction Kinetics of Gas-Phase α- and γ-Hexachlorocyclohexane and Hexachlorobenzene, Environ. Sci. Technol., 32, 766-769, 1998.

Carrera, G., Fernández, P., Grimalt, J. O., Ventura, M., Camarero, L., Catalan, J., Nickus, U., Thies, H., and Psenner, R.: Atmospherc deposition of organochlorine compounds to remote high mountain lakes of Europe, Environ. Sci. Technol., 36, 2581-2588, 2002.

Cetin, B., Ozer, S., Sofuoglu, A., and Odabasi, M.: Determination of Henry's law constants of organochlorine pesticides in deionized and saline water as a function of temperature, Atmos. Environ., 40, 4538-4546, doi: 10.1016/j.atmosenv.2006.04.009, 2006.

Chakraborty, P., Zhang, G., Li, J., Sivakumar, A., and Jones, K. C.: Occurrence and sources of selected organochlorine pesticides in the soil of seven major Indian cities: Assessment of air–soil exchange, Environ. Pollut., 204, 74-80, 2015.

Dalla Valle, M., Jurado, E., Dachs, J., Sweetman, A. J., and Jones, K. C.: The maximum reservoir capacity of soils for persistent organic pollutants: implications for global cycling, Environ. Pollut., 134, 153-164, doi: 10.1016/j.envpol.2004.07.011, 2005.

Daly, G. L., Lei, Y. D., Teixeira, C., Muir, D. C. G., and Wania, F.: Pesticides in western Canadian mountain air and soil, Environ. Sci. Technol., 41, 6020-6025, doi: 10.1021/Es070848o, 2007.

Ding, X., Wang, X. M., Xie, Z. Q., Xiang, C. H., Mai, B. X., Sun, L. G., Zheng, M., Sheng, G. Y., Fu, J. M., and Poschl, U.: Atmospheric polycyclic aromatic hydrocarbons observed over the North Pacific Ocean and the Arctic area: Spatial distribution and source identification, Atmos. Environ., 41, 2061-2072, doi:10.1016/j.atmonsenv.2006.11.002, 2007.

Fernandez, P., Grimalt, J. O., and Vilanova, R. M.: Atmospheric gas-particle partitioning of polycyclic aromatic hydrocarbons in high mountain regions of Europe, Environ. Sci. Technol., 36, 1162-1168, doi: 10.1021/Es010190t, 2002.

Franz, T. P., and Eisenreich, S. J.: Snow scavenging of polychlorinated biphenyls and polycyclic aromatic hydrocarbons in Minnesota, Environ. Sci. Technol., 32, 1771-1778, doi: 10.1021/Es970601z, 1998.

Froescheis, O., Looser, R., Cailliet, G. M., Jarman, W. M., and Ballschmiter, K.: The deep-sea as a final global sink of semivolatile persistent organic pollutants? Part I: PCBs in surface and deep-sea dwelling fish of the North and South Atlantic and the Monterey Bay Canyon (California), Chemosphere, 40, 651-660, doi: 10.1016/S0045-6535(99)00461-0, 2000.

Gioia, R., Lohmann, R., Dachs, J., Temme, C., Lakaschus, S., Schulz-Bull, D., Hand, I., and Jones, K. C.: Polychlorinated biphenyls in air and water of the North Atlantic and Arctic Ocean, J.

662   Geophys. Res., 113, doi: 10.1029/2007jd009750, 2008.

663   Gioia, R., Li, J., Schuster, J., Zhang, Y. L., Zhang, G., Li, X. D., Spiro, B., Bhatia, R. S., Dachs, J.,
664   and Jones, K. C.: Factors Affecting the Occurrence and Transport of Atmospheric
665   Organochlorines in the China Sea and the Northern Indian and South East Atlantic Oceans,
666   Environ. Sci. Technol., 46, 10012-10021, doi: 10.1021/Es302037t, 2012.

667   Gong, P., Wang, X. P., and Yao, T. D.: Ambient distribution of particulate- and gas-phase n-alkanes
668   and polycyclic aromatic hydrocarbons in the Tibetan Plateau, Environmental Earth Sciences,
669   64, 1703-1711, doi:10.1007/s12665-011-0974-3, 2011.

670   Gonzalez-Gaya, B., Zuniga-Rival, J., Ojeda, M. J., Jimenez, B., and Dachs, J.: Field
671   Measurements of the Atmospheric Dry Deposition Fluxes and Velocities of Polycyclic
672   Aromatic Hydrocarbons to the Global Oceans, Environ. Sci. Technol., 48, 5583-5592,
673   doi:10.1021/es500846p, 2014.

674   Gonzalez-Gaya, B., Fernandez-Pinos, M. C., Morales, L., Mejanelle, L., Abad, E., Pina, B., Duarte,
675   C. M., Jimenez, B., and Dachs, J.: High atmosphere-ocean exchange of semivolatile aromatic
676   hydrocarbons, Nature Geoscience, 9, 438-442, doi:10.1038/NGEO2714, 2016.

677   Guglielmo, F., Stemmler, I., and Lammel, G.: The impact of organochlorines cycling in the
678   cryosphere on their global distribution and fate-1. Sea ice, Environ. Pollut., 162, 475-481,
679   doi:10.1016/j.envpol.2011.09.039, 2012.

680   Guzzella, L., Poma, G., De Paolis, A., Roscioli, C., and Viviano, G.: Organic persistent toxic
681   substances in soils, waters and sediments along an altitudinal gradient at Mt. Sagarmatha,
682   Himalayas, Nepal, Environ. Pollut., 159, 2552-2564, doi:10.1016/j.envpol.2011.06.015,
683   2011.

684   Geisz, H. N., Dickhut, R. M., Cochran, M. A., Fraser, W. R., and Ducklow, H. W.: Melting
685   glaciers: A probable source of DDT to the Antarctic marine ecosystem, Environ. Sci. Technol.,
686   42, 3958-3962, doi:10.1021/es702919n, 2008.

687   Harner, T., Wiberg, K., and Norstrom, R.: Enantiomer fractions are preferred to enantiomer ratios
688   for describing chiral signatures in environmental analysis, Environ. Sci. Technol., 34,
689   218-220, 2000.

690   Hu, T., Cao, J., Lee, S., Ho, K., Li, X., Liu, S., and Chen, J.: Physiochemical characteristics of
691   indoor PM2.5 with combustion of dried yak dung as biofuel in Tibetan Plateau, China, Indoor
692   & Built Environment, 191, 172-181, 2015.

693   Huang, Y. M., Xu, Y., Li, J., Xu, W. H., Zhang, G., Cheng, Z. N., Liu, J. W., Wang, Y., and Tian, C.
694   G.: Organochlorine Pesticides in the Atmosphere and Surface Water from the Equatorial
695   Indian Ocean: Enantiomeric Signatures, Sources, and Fate, Environ. Sci. Technol., 47,
696   13395-13403, doi: 10.1021/Es403138p, 2013.

697   Hung, H., Kallenborn, R., Breivik, K., Su, Y. S., Brorstrom-Lunden, E., Olafsdottir, K., Thorlacius,
698   J. M., Leppanen, S., Bossi, R., Skov, H., Mano, S., Patton, G. W., Stern, G., Sverko, E., and
699   Fellin, P.: Atmospheric monitoring of organic pollutants in the Arctic under the Arctic
700   Monitoring and Assessment Programme (AMAP): 1993-2006, Sci. Total Environ., 408,
701   2854-2873, doi: 10.1016/j.scitotenv.2009.10.044, 2010.

702   Iwata, H., Tanabe, S., Sakal, N., and Tatsukawa, R.: Distribution of Persistent Organochlorines in
703   the Oceanic Air and Surface Seawater and the Role of Ocean on Their Global Transport and
704   Fate, Environ. Sci. Technol., 27, 1080-1098, 1993.

705   Jantunen, L. M., Helm, P. A., Kylin, H., and Bidlemant, T. F.: Hexachlorocyclohexanes (HCHs) in

706   the Canadian archipelago. 2. Air-water gas exchange of alpha- and gamma-HCH, Environ.
707   Sci. Technol., 42, 465-470, doi: 10.1021/Es071646v, 2008.

708 Jantunen, L. M., Wong, F., Gawor, A., Kylin, H., Helm, P. A., Stern, G. A., Strachan, W. M. J.,
709   Burniston, D. A., and Bidleman, T. F.: 20 Years of Air-Water Gas Exchange Observations for
710   Pesticides in the Western Arctic Ocean, Environ. Sci. Technol., 49, 13844-13852,
711   doi:10.1021/acs.est.5b01303, 2015.

712 Jurado, E., Jaward, F., Lohmann, R., Jones, K. C., Simo, R., and Dachs, J.: Wet deposition of
713   persistent organic pollutants to the global oceans, Environ. Sci. Technol., 39, 2426-2435, doi:
714   10.1021/Es048599g, 2005.

715 Kang, J. H., Choi, S. D., Park, H., Baek, S. Y., Hong, S., and Chang, Y. S.: Atmospheric deposition
716   of persistent organic pollutants to the East Rongbuk Glacier in the Himalayas, Sci. Total
717   Environ., 408, 57-63, doi:10.1016/j.scitotenv.2009.09.015, 2009.

718 Keyte, I. J., Harrison, R. M., and Lammel, G.: Chemical reactivity and long-range transport
719   potential of polycyclic aromatic hydrocarbons - a review, Chemical Society Reviews, 42,
720   9333-9391, doi:10.1039/c3cs60147a, 2013.

721 Khairy, M., Muir, D., Teixeira, C., and Lohmann, R.: Spatial Trends, Sources, and Air-Water
722   Exchange of Organochlorine Pesticides in the Great Lakes Basin Using Low Density
723   Polyethylene Passive Samplers, Environ. Sci. Technol., 48, 9315-9324,
724   doi:10.1021/es501686a, 2014.

725 Komprda, J., Komprdova, K., Sanka, M., Mozny, M., and Nizzetto, L.: Influence of Climate and
726   Land Use Change on Spatially Resolved Volatilization of Persistent Organic Pollutants (POPs)
727   from Background Soils, Environ. Sci. Technol., 47, 7052-7059, doi:10.1021/es30437134,
728   2013.

729 Kurt-Karakus, P. B., Bidleman, T. F., Staebler, R. M., and Jones, K. C.: Measurement of DDT
730   fluxes from a historically treated agricultural soil in Canada, Environ. Sci. Technol., 40,
731   4578-4585, doi: 10.1021/Es060216m, 2006.

732 Law, S. A., Diamond, M. L., Helm, P. A., Jantunen, L. M., and Alaee, M.: Factors affecting the
733   occurrence and enantiomeric degradation of hexachlorocyclohexane isomers in northern and
734   temperate aquatic systems, Environ. Toxicol. Chem., 20, 2690–2698, 2001.

735 Leys, N. M., Ryngaert, A., Bastiaens, L., Top, E. M., Verstraete, W., and Springael, D.: Culture
736   Independent Detection of Sphingomonas sp. EPA 505 Related Strains in Soils Contaminated
737   with Polycyclic Aromatic Hydrocarbons (PAHs), Microb. Ecol., 49, 443-450, 2005.

738 Li, C. L., Kang, S. C., Chen, P. F., Zhang, Q. G., and Fang, G. C.: Characterizations of
739   particle-bound trace metals and polycyclic aromatic hydrocarbons (PAHs) within Tibetan
740   tents of south Tibetan Plateau, China, Environ Sci Pollut Res, 19, 1620-1628,
741   doi:10.1007/s11356-011-0678-y, 2012.

742 Li, C. L., Bosch, C., Kang, S. C., Andersson, A., Chen, P. F., Zhang, Q. G., Cong, Z. Y., Chen, B.,
743   Qin, D. H., and Gustafsson, O.: Sources of black carbon to the Himalayan-Tibetan Plateau
744   glaciers, Nature Communications, 7, doi: 10.1038/Ncomms12574, 2016.

745 Li, J., Zhu, T., Wang, F., Qiu, X. H., and Lin, W. L.: Observation of organochlorine pesticides in
746   the air of the Mt. Everest region, Ecotoxicol. Environ. Saf., 63, 33-41, doi:
747   10.1016/j.ecoenv.2005.04.001, 2006.

748 Liu, X., and Chen, B.: Climatic warming in the Tibetan Plateau during recent decades,
749   International Journal of Climatology, 20, 1729–1742, 2000.

Liu, X. B., Yao, T. D., Kang, S. C., Jiao, N. A. Z., Zeng, Y. H., and Liu, Y. Q.: Bacterial Community of the Largest Oligosaline Lake, Namco on the Tibetan Plateau, Geomicrobiol. J., 27, 669-682, doi: 10.1080/01490450903528000, 2010.

Liu, Y. Q., Yao, T. D., Jiao, N. Z., Kang, S. C., Xu, B. Q., Zeng, Y. H., Huang, S. J., and Liu, X. B.: Bacterial diversity in the snow over Tibetan Plateau Glaciers, Extremophiles, 13, 411-423, doi:10.1007/s00792-009-0227-5, 2009.

Liu, Y. Q., Yao, T. D., Jiao, N. Z., Liu, X. B., Kang, S. C., and Luo, T. W.: Seasonal Dynamics of the Bacterial Community in Lake Namco, the Largest Tibetan Lake, Geomicrobiol. J., 30, 17-28, doi:10.1080/01490451.2011.638700, 2013.

Lohmann, R., Gioia, R., Jones, K. C., Nizzetto, L., Temme, C., Xie, Z., Schulz-Bull, D., Hand, I., Morgan, E., and Jantunen, L.: Organochlorine Pesticides and PAHs in the Surface Water and Atmosphere of the North Atlantic and Arctic Ocean, Environ. Sci. Technol., 43, 5633-5639, doi: 10.1021/Es901229k, 2009.

Ma, J. M., Hung, H. L., Tian, C., and Kallenborn, R.: Revolatilization of persistent organic pollutants in the Arctic induced by climate change, Nature Climate Change, 1, 255-260, doi: 10.1038/Nclimate1167, 2011.

Ma, Y. G., Lei, Y. D., Xiao, H., Wania, F., and Wang, W. H.: Critical Review and Recommended Values for the Physical-Chemical Property Data of 15 Polycyclic Aromatic Hydrocarbons at 25 degrees C, J. Chem. Eng. Data., 55, 819-825, doi: 10.1021/Je900477x, 2010.

Ma, Y. X., Xie, Z. Y., Yang, H. Z., Moller, A., Halsall, C., Cai, M. H., Sturm, R., and Ebinghaus, R.: Deposition of polycyclic aromatic hydrocarbons in the North Pacific and the Arctic, J. Geophys. Res., 118, 5822-5829, doi:10.1002/jgrd.50473, 2013.

Mulder, M. D., Heil, A., Kukucka, P., Klanova, J., Kuta, J., Prokes, R., Sprovieri, F., and Lammel, G.: Air-sea exchange and gas-particle partitioning of polycyclic aromatic hydrocarbons in the Mediterranean, Atmospheric Chemistry and Physics, 14, 8905-8915, doi:10.5194/acp-14-8905-2014, 2014.

Nizzetto, L., Lohmann, R., Gioia, R., Jahnke, A., Temme, C., Dachs, J., Herckes, P., Di, G. A., and Jones, K. C.: PAHs in air and seawater along a North-South Atlantic transect: trends, processes and possible sources, Environ. Sci. Technol., 42, 1580-1585, 2008.

Noyes, P. D., McElwee, M. K., Miller, H. D., Clark, B. W., Van Tiem, L. A., Walcott, K. C., Erwin, K. N., and Levin, E. D.: The toxicology of climate change: Environmental contaminants in a warming world, Environ. Int., 35, 971-986, doi:10.1016/j.envint.2009.02.006, 2009.

Ridal, J. J., Bidleman, T. F., Kerman, B. R., Fox, M. E., and Strachan, W. M. J.: Enantiomers of alpha-hexachlorocyclohexane as tracers of air-water gas exchange in Lake Ontario, Environ. Sci. Technol., 31, 1940-1945, doi: 10.1021/Es9607244, 1997.

Ruzickova, P., Klanova, J., Cupr, P., Lammel, G., and Holoubek, I.: An assessment of air-soil exchange of polychlorinated biphenyls and organochlorine pesticides across Central and Southern Europe, Environ. Sci. Technol., 42, 179-185, doi: 10.1021/Es071406f, 2008.

Sheng, J. J., Wang, X. P., Gong, P., Joswiak, D. R., Tian, L. D., Yao, T. D., and Jones, K. C.: Monsoon-driven transport of organochlorine pesticides and polychlorinated biphenyls to the tibetan plateau: three year atmospheric monitoring study, Environ. Sci. Technol., 47, 3199-3208, doi:10.1021/es305201s, 2013.

Spivakovsky, C. M., Logan, J. A., Montzka, S. A., Balkanski, Y. J., Foreman-Fowler, M., Jones, D. B. A., Horowitz, L. W., Fusco, A. C., Brenninkmeijer, C. A. M., and Prather, M. J.:

Three-dimensional climatological distribution of tropospheric OH: Update and evaluation, J. Geophys. Res., 105, 8931–8980, 2000.

Stemmler, I., and Lammel, G.: Cycling of DDT in the global environment 1950-2002: World ocean returns the pollutant, Geophys. Res. Lett., 36, doi:10.1029/2009GL041340, 2009.

Su, Y. S., Hung, H., Blanchard, P., Patton, G. W., Kallenborn, R., Konoplev, A., Fellin, P., Li, H., Geen, C., Stern, G., Rosenberg, B., and Barrie, L. A.: A circumpolar perspective of atmospheric organochlorine pesticides (OCPs): Results from six Arctic monitoring stations in 2000-2003, Atmos. Environ., 42, 4682-4698, doi:10.1016/j.atmosenv.2008.01.054, 2008.

Su, Y. S., Hung, H., Blanchard, P., Patton, G. W., Kallenborn, R., Konoplev, A., Fellin, P., Li, H., Geen, C., Stern, G., Rosenberg, B., and Barrie, L. A.: Spatial and seasonal variations of hexachlorocyclohexanes (HCHs) and hexachlorobenzene (HCB) in the Arctic atmosphere, Environ. Sci. Technol., 40, 6601-6607, doi: 10.1021/Es061065q, 2006.

Tranvik, L. J., Downing, J. A., Cotner, J. B., Loiselle, S. A., Striegl, R. G., Ballatore, T. J., Dillon, P., Finlay, K., Fortino, K., Knoll, L. B., Kortelainen, P. L., Kutser, T., Larsen, S., Laurion, I., Leech, D. M., McCallister, S. L., McKnight, D. M., Melack, J. M., Overholt, E., Porter, J. A., Prairie, Y., Renwick, W. H., Roland, F., Sherman, B. S., Schindler, D. W., Sobek, S., Tremblay, A., Vanni, M. J., Verschoor, A. M., von Wachenfeldt, E., and Weyhenmeyer, G. A.: Lakes and reservoirs as regulators of carbon cycling and climate, Limnol. Oceanogr., 54, 2298-2314, doi: 10.4319/lo.2009.54.6_part_2.2298, 2009.

Tremolada, P., Villa, S., Bazzarin, P., Bizzotto, E., Comolli, R., and Vighi, M.: POPs in Mountain Soils from the Alps and Andes: Suggestions for a 'Precipitation Effect' on Altitudinal Gradients, Water Air & Soil Pollution, 188, 93-109, 2008.

Venier, M., Dove, A., Romanak, K., Backus, S., and Hites, R.: Flame Retardants and Legacy Chemicals in Great Lakes' Water, Environ. Sci. Technol., 48, 9563-9572, doi:10.1021/es501509r, 2014.

Vilanova, R. M., Fernandez, P., Martinez, C., and Grimalt, J. O.: Polycyclic aromatic hydrocarbons in remote mountain lake waters, Water Res., 35, 3916-3926, doi: 10.1016/S0043-1354(01)00113-0, 2001.

Wang, C. F., Wang, X. P., Gong, P., and Yao, T. D.: Polycyclic aromatic hydrocarbons in surface soil across the Tibetan Plateau: Spatial distribution, source and air-soil exchange, Environ. Pollut., 184, 138-144, doi:10.1016/j.envpol.2013.08.029, 2014.

Wang, J. B., Zhu, L. P., Daut, G., Ju, J. T., Lin, X., Wang, Y., and Zhen, X. L.: Investigation of bathymetry and water quality of Lake Nam Co, the largest lake on the central Tibetan Plateau, China, Limnology, 10, 149-158, doi:10.1007/s10201-009-0266-8, 2009.

Wang, X. P., Gong, P., Wang, C. F., Ren, J., and Yao, T. D.: A review of current knowledge and future prospects regarding persistent organic pollutants over the Tibetan Plateau, Sci. Total Environ., 573, 139-154, doi: org/10.1016/j.scitotenv.2016.08.107, 2016.

Wang, X. P., Sheng, J. J., Gong, P., Xue, Y. G., Yao, T. D., and Jones, K. C.: Persistent organic pollutants in the Tibetan surface soil: Spatial distribution, air-soil exchange and implications for global cycling, Environ. Pollut., 170, 145-151, doi: 10.1016/j.envpol.2012.06.012, 2012.

Wang, X. P., Gong, P., Sheng, J. J., Joswiak, D. R., and Yao, T. D.: Long-range atmospheric transport of particulate Polycyclic Aromatic Hydrocarbons and the incursion of aerosols to the southeast Tibetan Plateau, Atmos. Environ., 115, 124-131, doi:10.1016/j.atmosenv.2015.04.050, 2015.

838 Wania, F., Axelman, J., and Broman, D.: A review of processes involved in the exchange of
839   persistent organic pollutants across the air-sea interface, Environ. Pollut., 102, 3-23, doi:
840   10.1016/S0269-7491(98)00072-4, 1998a.
841 Wania, F., Haugen, J. E., Lei, Y. D., and Mackay, D.: Temperature dependence of atmospheric
842   concentrations of semivolatile organic compounds, Environ. Sci. Technol., 32, 1013-1021,
843   doi: 10.1021/Es970856c, 1998b.
844 Wania, F., Hoff, J. T., Jia, C. Q., and Mackay, D.: The effects of snow and ice on the
845   environmental behaviour of hydrophobic organic chemicals, Environ. Pollut., 102, 25-41, doi:
846   10.1016/S0269-7491(98)00073-6, 1998c.
847 Wilkinson, A. C., Kimpe, L. E., and Blais, J. M.: Air-water gas exchange of chlorinated pesticides
848   in four lakes spanning a 1,205 meter elevation range in the Canadian Rocky Mountains,
849   Environ. Toxicol. Chem., 24, 61-69, doi: 10.1897/04-071r.1, 2005.
850 Wong, F., Jantunen, L. M., Pucko, M., Papakyriakou, T., Staebler, R. M., Stern, G. A., and
851   Bidleman, T. F.: Air-Water Exchange of Anthropogenic and Natural Organohalogens on
852   International Polar Year (IPY) Expeditions in the Canadian Arctic, Environ. Sci. Technol., 45,
853   876-881, doi: 10.1021/Es1018509, 2011.
854 Wu, Y. H., Zheng, H. X., Zhang, B., Chen, D. M., and Lei, L. P.: Long-Term Changes of Lake
855   Level and Water Budget in the Nam Co Lake Basin, Central Tibetan Plateau, Journal of
856   Hydrometeorology, 15, 1312-1322, doi:10.1175/Jhm-D-13-093.1, 2014.
857 Xiao, H., Kang, S. C., Zhang, Q. G., Han, W. W., Loewen, M., Wong, F., Hung, H., Lei, Y. D., and
858   Wania, F.: Transport of semivolatile organic compounds to the Tibetan Plateau: Monthly
859   resolved air concentrations at Nam Co, J. Geophys. Res., 115, doi: 10.1029/2010jd013972,
860   2010.
861 Xiao, Q. Y., Saikawa, E., Yokelson, R. J., Chen, P. F., Li, C. L., and Kang, S. C.: Indoor air
862   pollution from burning yak dung as a household fuel in Tibet, Atmos. Environ., 102, 406-412,
863   doi:10.1016/j.atmosenv.2014.11.060, 2015.
864 Yang, R. Q., Xie, T., An, L., Yang, H., Turner, S., Wu, G., and Jing, C.: Sedimentary records of
865   polycyclic aromatic hydrocarbons (PAHs) in remote lakes across the Tibetan Plateau,
866   Environ. Pollut., 214, 1-7, 2016.
867 Yao, T. D., Thompson, L. G., Mosbrugger, V., Zhang, F., Ma, Y., Luo, T., Xu, B. Q., Yang, X.,
868   Joswiak, D. R., Wang, W., Joswiak, M. E., Devkota, L. P., Tayal, S., Jilani, R., and Fayziev,
869   R.: Third Pole Environment (TPE), Environmental Development, 3, 52-64,
870   doi:10.1016/j.envdev.2012.04.002, 2012.
871 Zhang, G., Chakraborty, P., Li, J., Sampathkumar, P., Balasubramanian, T., Kathiresan, K.,
872   Takahashi, S., Subramanian, A., Tanabe, S., and Jones, K. C.: Passive Atmospheric Sampling
873   of Organochlorine Pesticides, Polychlorinated Biphenyls, and Polybrominated Diphenyl
874   Ethers in Urban, Rural, and Wetland Sites along the Coastal Length of India, Environ. Sci.
875   Technol., 42, 8218-8223, doi: 10.1021/Es8016667, 2008.
876 Zhang, G. Q., Yao, T. D., Xie, H. J., Zhang, K. X., and Zhu, F. J.: Lakes' state and abundance
877   across the Tibetan Plateau, Chin. Sci. Bull., 59, 3010-3021, doi:10.1007/s11434-014-0258-x,
878   2014.
879 Zhang, W. L., Zhang, G., Qi, S. H. and Peng, P. A.: A preliminary study of
880   organochlorinepesticides in water and sediments from two Tibetan Lakes. Geochimica. 32 (4),
881   363-367 (in Chinese with English abstract), 2003.

Table 1. Estimated fluxes (ng m^{-2} day^{-1}) of air-water gas exchange (F_{AW}), atmospheric degradation (F_{deg}), dry deposition (F_{DD}), and wet deposition (F_{WD}) for individual PAHs during the ablation period and frozen periods, respectively.

PAH	ablation period				PAH	frozen period		
	F_{AW}	F_{deg}	F_{DD}	F_{WD}		F_{deg}	F_{DD}	F_{WD}
Volatilization compounds								
Acel	80 ±49	6 ±5	NA	-0.2 ±0.1	Acel	1 ±0.7	-0.02 ±0.001	-0.03 ±0.1
Ace	51 ±19	4 ±4	-0.003 ±0.002	-0.4 ±0.3	Ace	0.9 ±0.5	-0.01 ±0.01	-6 ±5
Flu	203 ±162	11 ±8	-0.1 ±0.02	-9 ±7	Flu	1.8 ±0.9	-0.2 ±0.2	-43 ±30
sum	**335**	**21**	**-0.1**	**-9**	**sum**	**4**	**-0.2**	**-49**
Phe	-340 ±604	82 ±67	-0.5 ±0.1	-42 ±35	Phe	10 ±4	-2.2 ±1.2	-345 ±237
Ant	NA	60 ±63	-0.04 ±0.03	-5 ±5	Ant	4 ±2	-0.11 ±0.05	-16 ±14
Fla	NA	5 ±5	-0.5 ±0.1	-20 ±18	Fla	0.5 ±0.3	-4.6 ±2.8	-93 ±64
Deposition compounds								
Pyr	-145 ±154	20 ±21	-0.4 ±0.1	-18 ±17	Pyr	2 ±1	-3 ±1.5	-128 ±83
BaA	-19 ±23	NA	-0.1 ±0.1	-3 ±4	BaA	NA	-1.1 ±0.5	-15 ±10
Chr	-54 ±62	7 ±8	-0.5 ±0.3	-47 ±56	Chr	0.2 ±0.1	-4.7 ±2.3	-19 ±13
Bbf	-5 ±3	0.2 ±0.1	-0.6 ±0.5	-6 ±5	Bbf	0.02 ±0.01	-2.2 ±3.2	-4 ±8
Bkf	-2 ±1	0.2 ±0.1	-0.4 ±0.4	-2 ±1	Bkf	0.1 ±0.04	-3.8 ±1.9	-8 ±5
Bap	-2 ±1	0.2 ±0.2	-0.3 ±0.5	-3 ±1	Bap	0.04 ±0.03	-4.7 ±2.3	-16 ±10
IcdP	-2 ±1	0.7 ±0.5	NA	-2 ±2	IcdP	0.1 ±0.1	NA	-3 ±6
DahA	-1 ±0.7	0.1 ±0.1	NA	-0.1 ±0.2	DahA	0.01 ±0.01	NA	-0.6 ±1
BghiP	-2 ±0.4	0.02 ±0.01	-1 ±1	-3 ±1	BghiP	0.01 ±0.01	-12 ±6	-6 ±3
sum	**-231**	**28**	**-3**	**-85**	**sum**	**2**	**-31**	**-199**
Total PAHs	\	**196**	**-4.5**	**-161**	**Total PAHs**	**20**	**-38**	**-702**

884 NA: not available; For F_{AW}, F_{DD} and F_{WD}, positive values indicate volatilization, and negative values indicate net deposition.

(a)
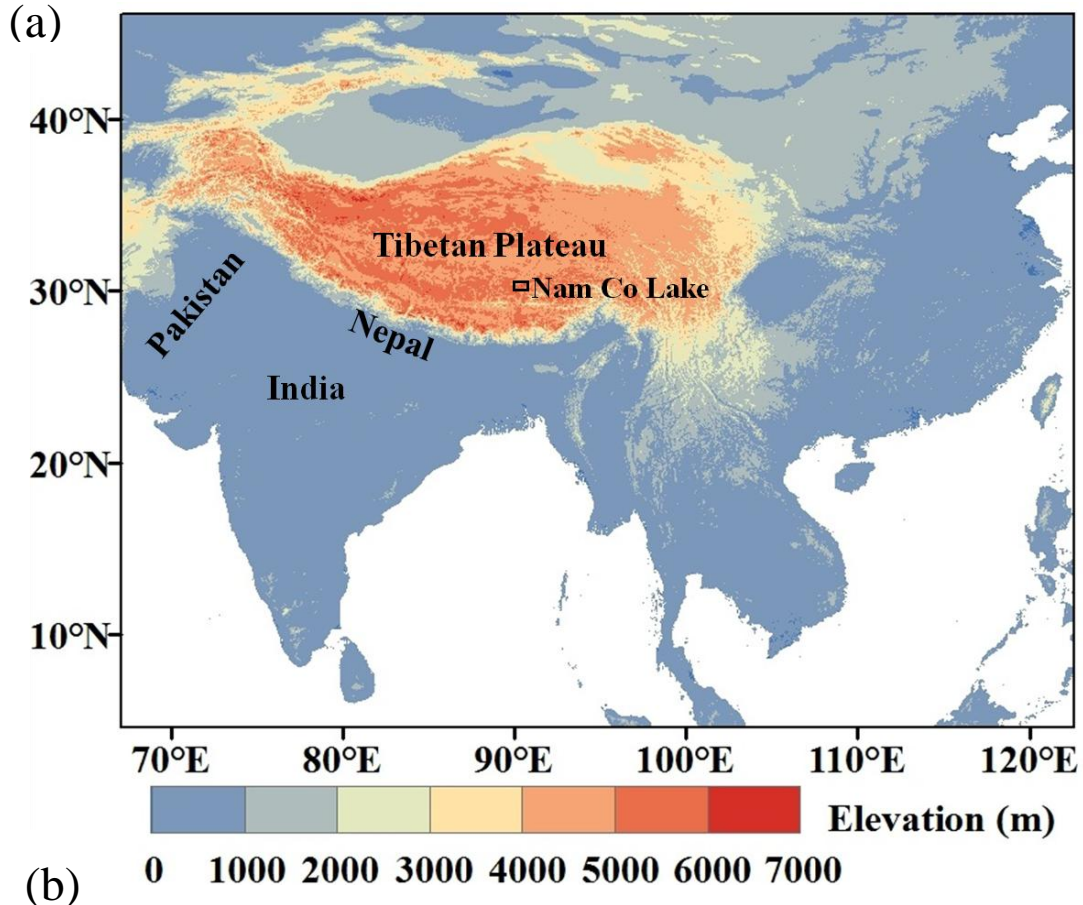
885   (b)
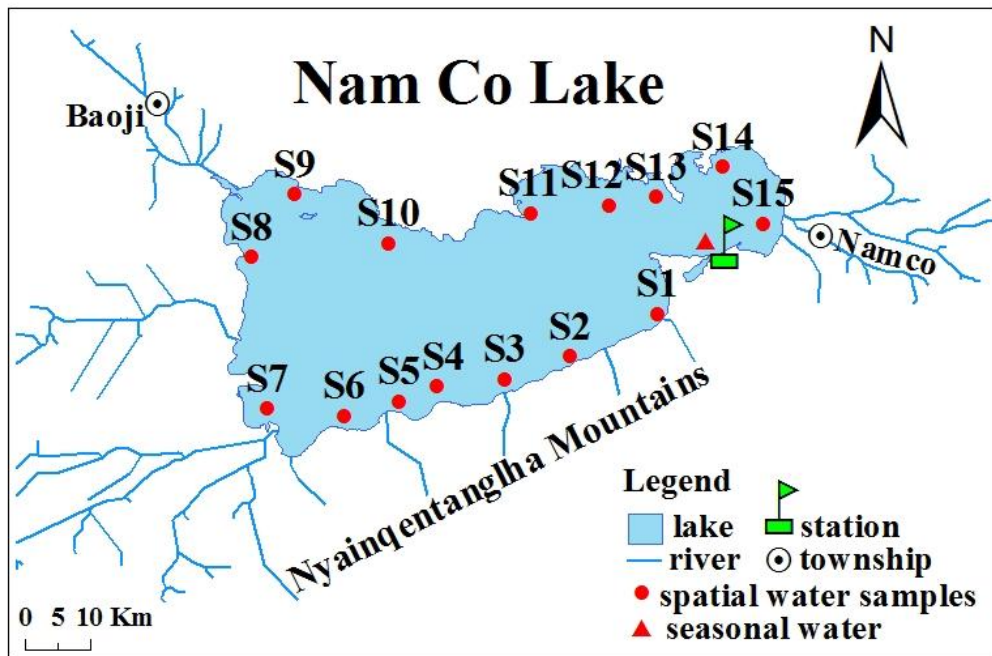
886

887   **Figure 1. Location of Nam Co Lake on the Tibetan Plateau (a) and the sampling**
888   **sites for air and lake water (b). The station refers to the Nam Co Monitoring and**
889   **Research Station, and it is also the air sampling site; S01 to S15 represent the 15**
890   **sampling sites of surface water around the lake; the red triangle represents the**
891   **sampling site of seasonal water from May to September.**
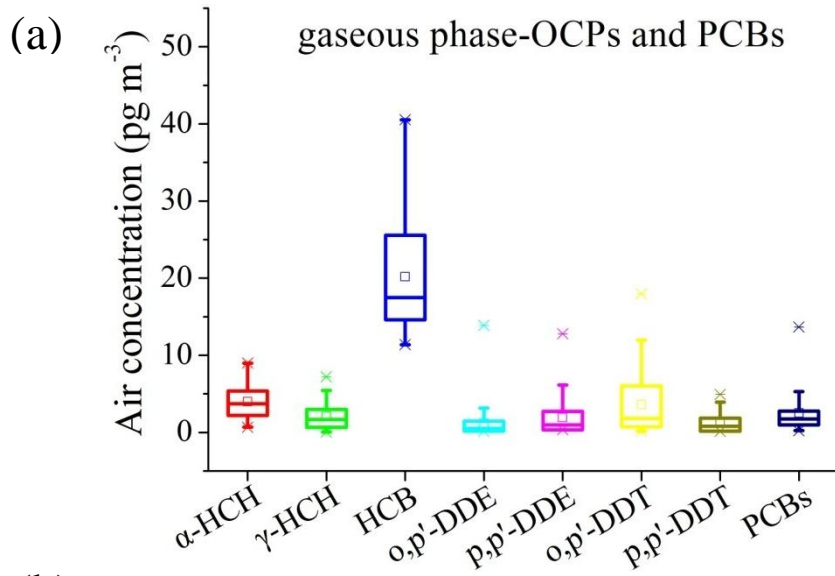
892
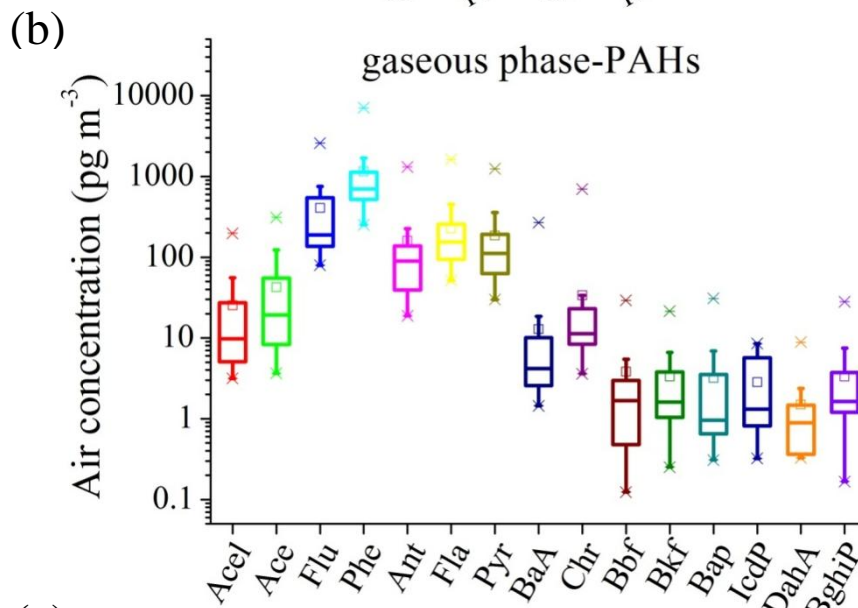
893
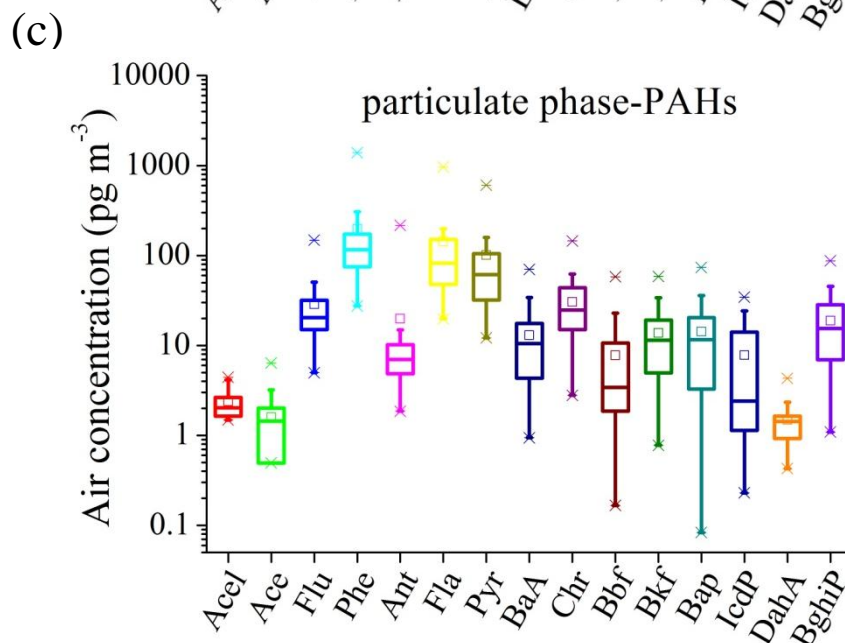
894

895 **Figure 2. Air concentrations of gaseous OCPs and PCBs (a), gaseous PAHs (b),**
896 **and particulate phase PAHs (c) in Nam Co. The boxes are defined by the 25th**

897 **and 75th percentiles; whiskers mark the 10th and 90th percentiles; the median is**
898 **represented by a horizontal line; the mean by a square; and outliers with an**
899 **asterisk.**

900
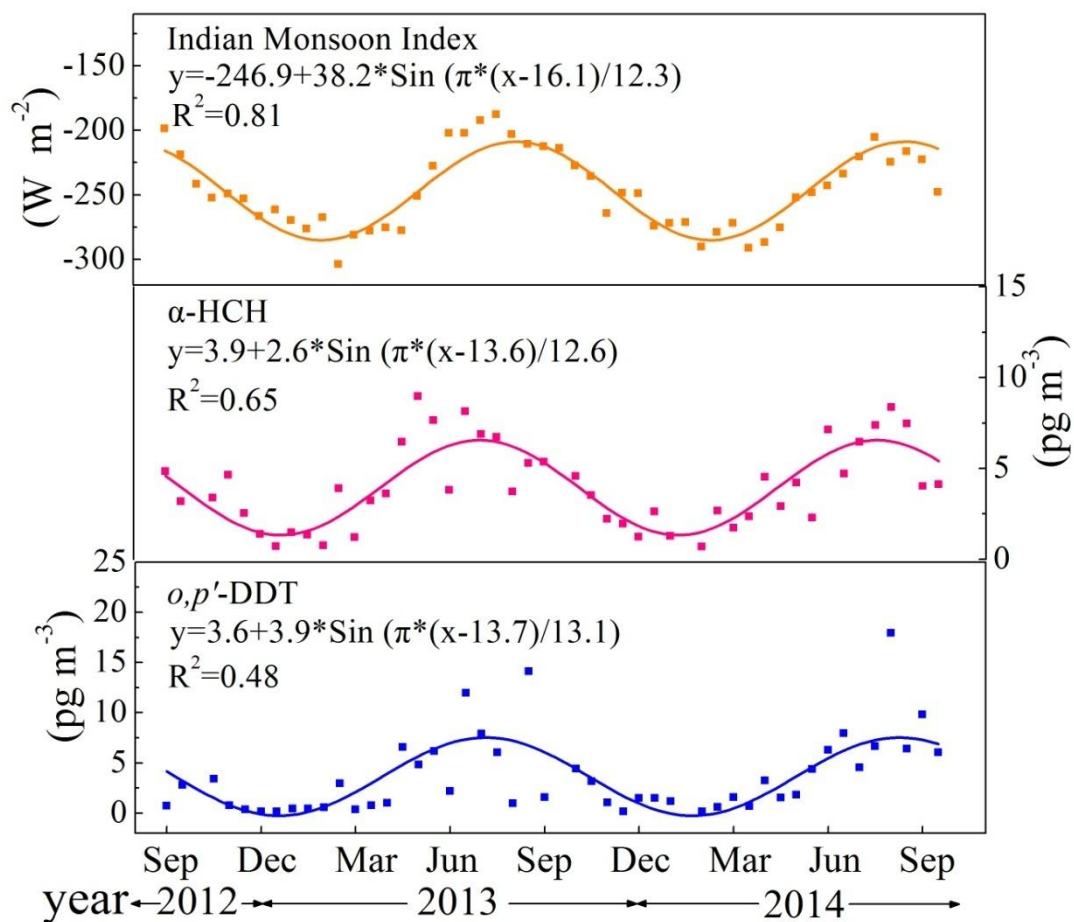
Figure 3. Seasonal patterns of Indian Monsoon Index, the atmospheric concentrations of α-HCH and *o,p′*-DDT.

901

902
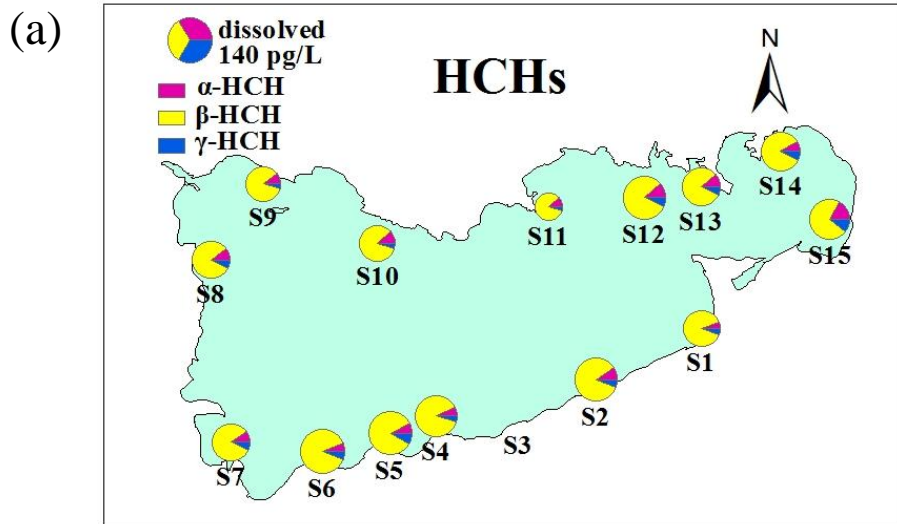
903
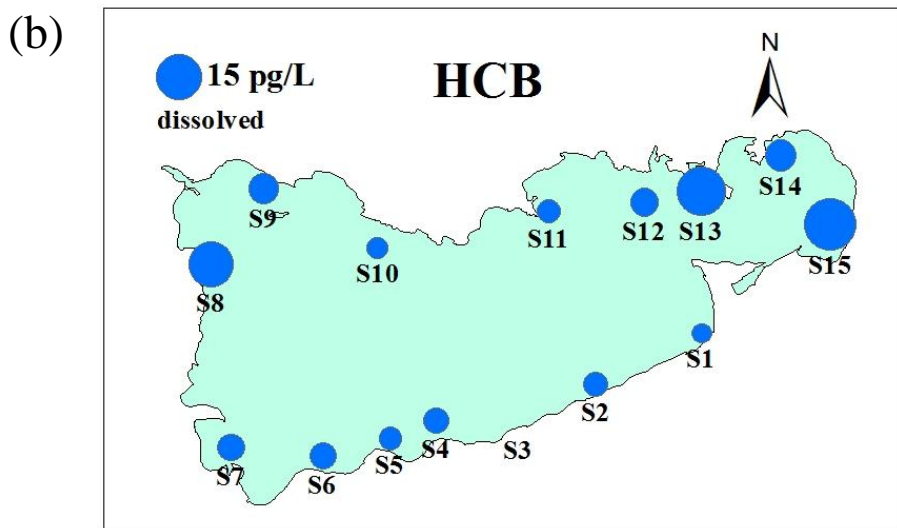
904
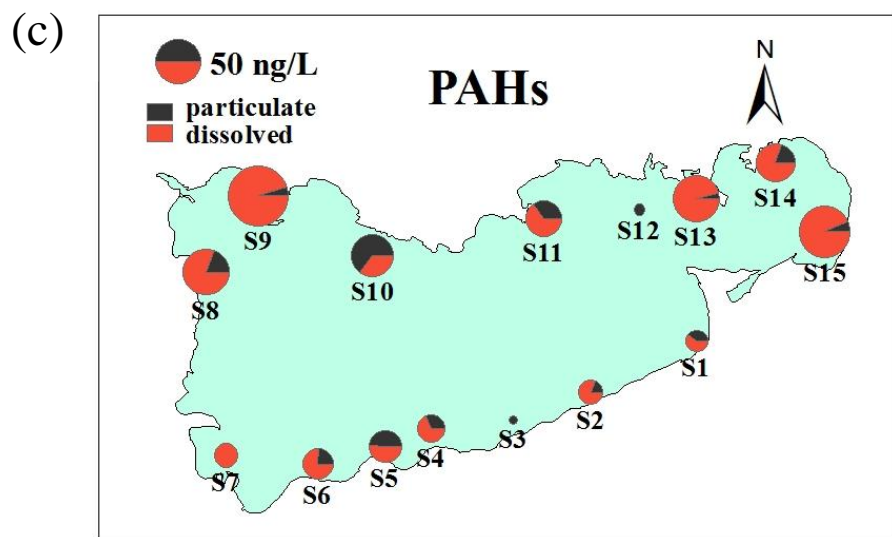
905

906 **Figure 4. Spatial distribution pattern of HCHs (a), HCB (b), and PAHs (c) in the**

907 **surface water of Nam Co Lake.**

(a)

908

(b)
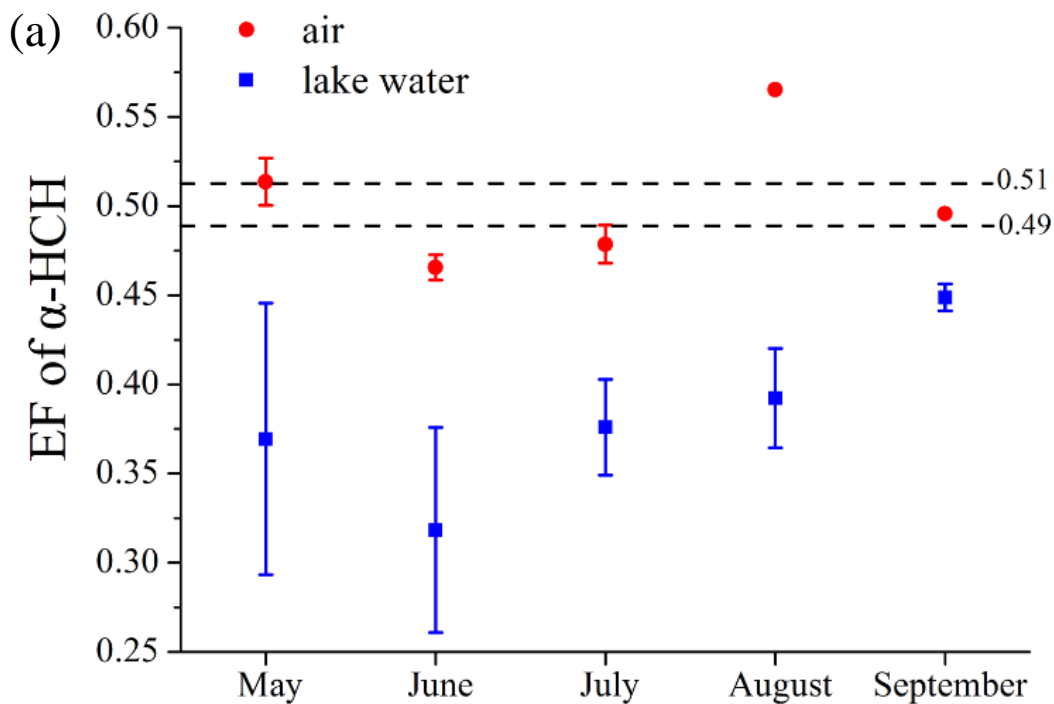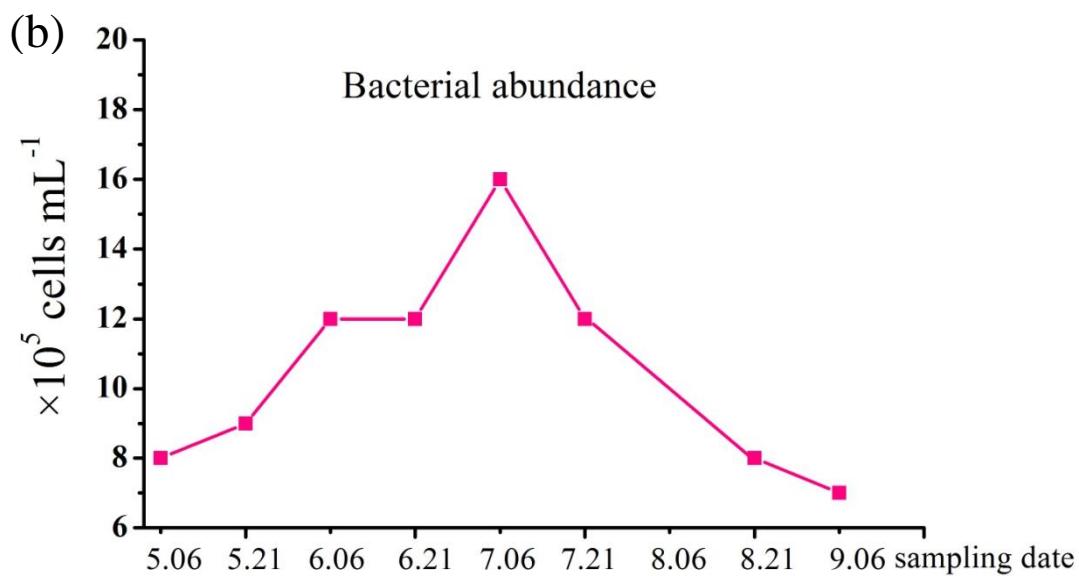
909

910 **Figure 5. Enantiomer fraction (EF) of α-HCH in the air and surface water from**

911 **May to September (a), and the seasonal bacterial abundance in Nam Co Lake**

912 **water (b). The data of bacterial abundance was derived from Liu et al. (2013),**

913 **which represents the total bacteria in the lake surface water.**

914

915

916
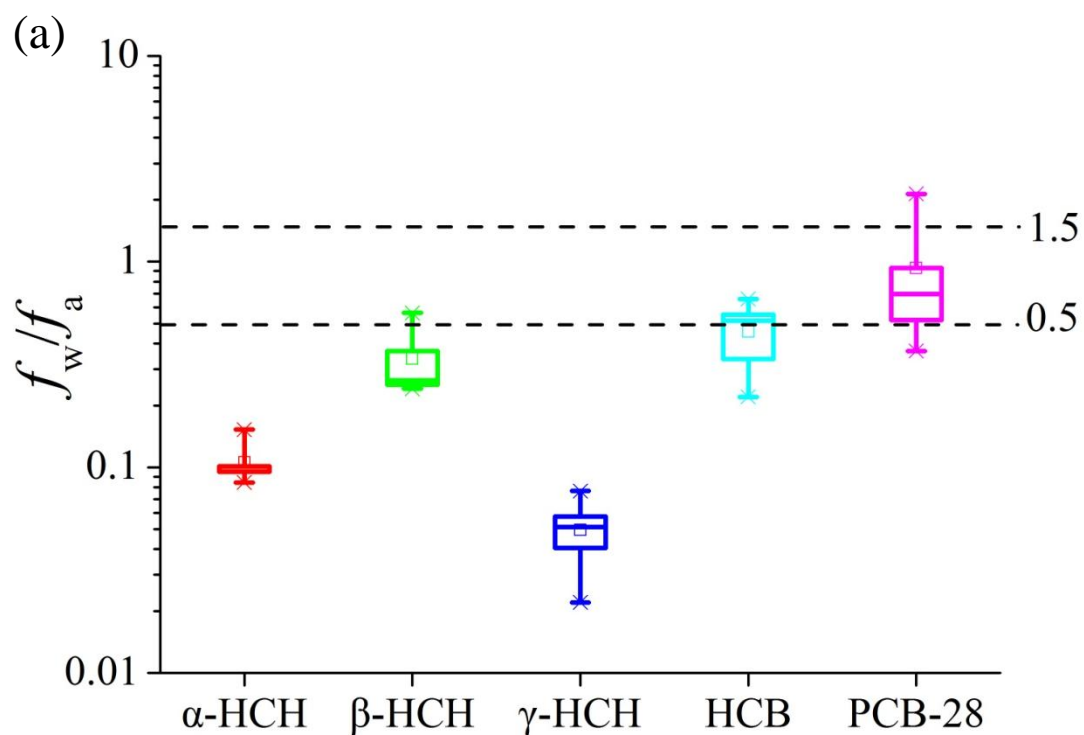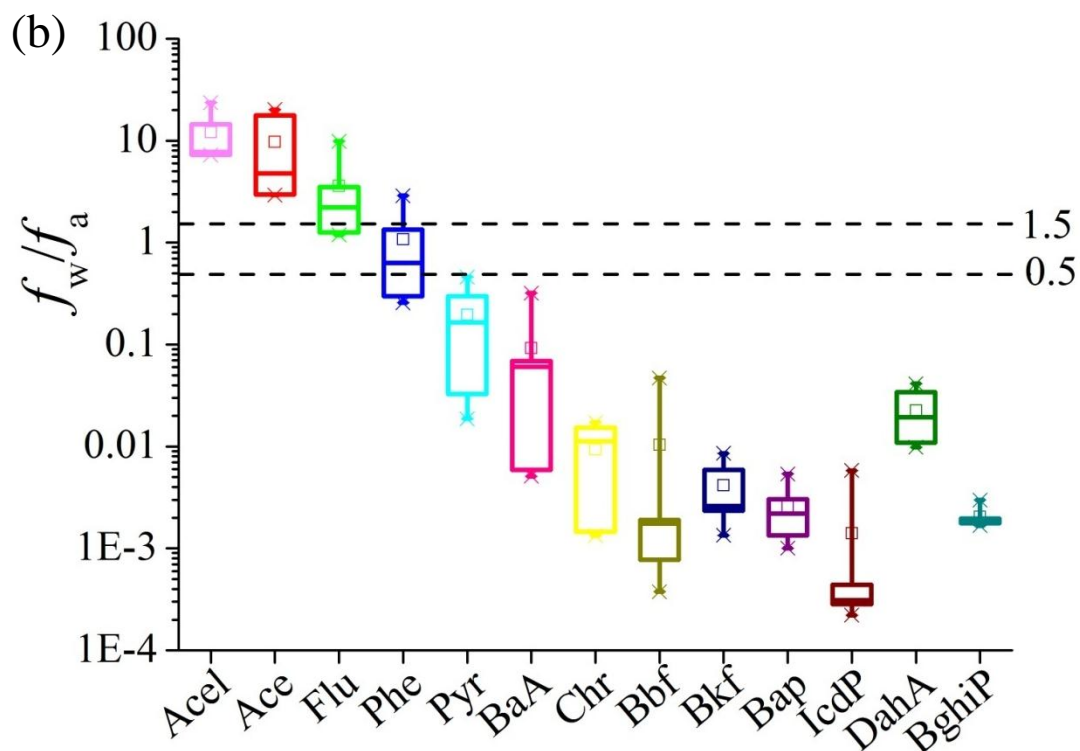
Figure 6. Water/air fugacity ratios (f_w/f_a) for OCPs and PCB 28 (a), and individual PAHs (b) in Nam Co Lake. The horizontal lines represent the uncertainty range, 0.5-1.5 was considered as equilibrium.

920

921

922
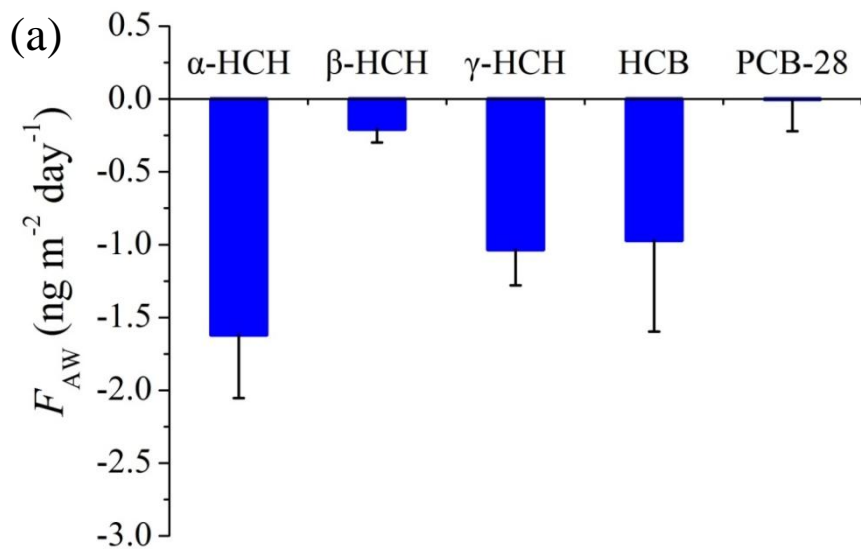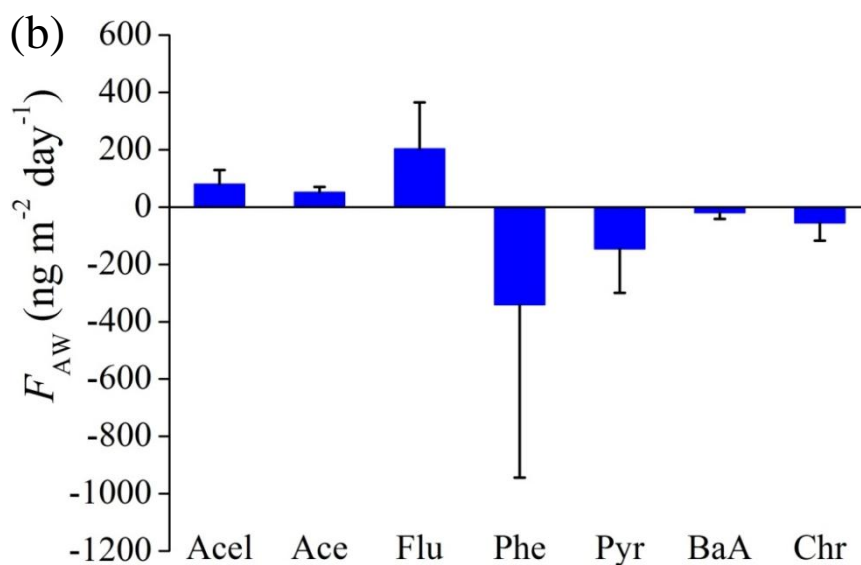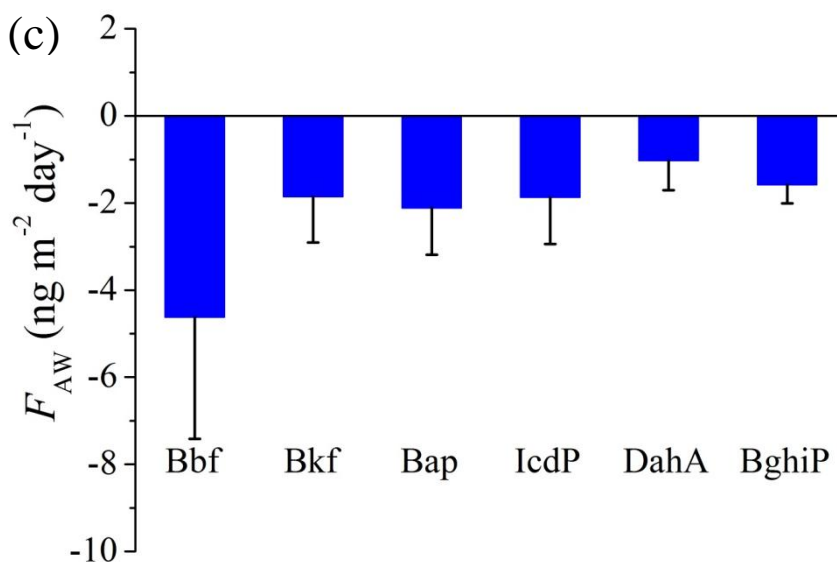
Figure 7. Average air-water gas exchange fluxes (F_{AW}) for individual OCPs, PCB 28 (a), and PAHs (b, c) in Nam Co Lake. Positive values indicate net volatilization, and negative values indicate net deposition.
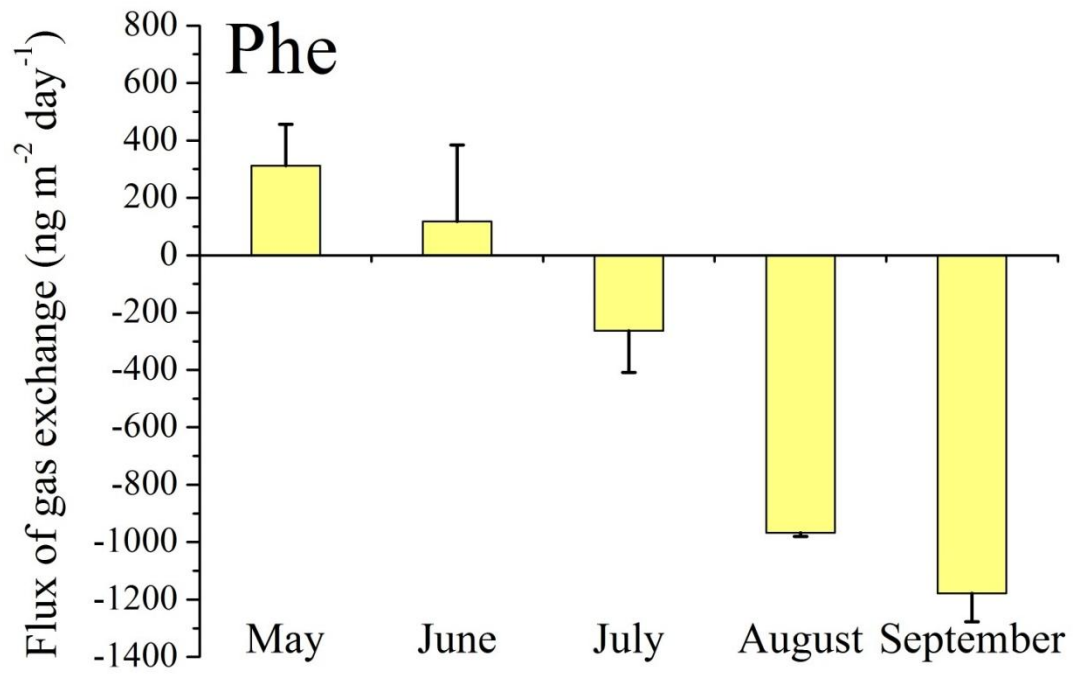
926

927 **Figure 8. Reversal of the air-water gas exchange for Phe from May to September.**